Die approbierte Originalversion dieser Diplom-/Masterarbeit ist in der Hauptbibliothek der Technischen Universität Wien aufgestellt und zugänglich.
http://www.ub.tuwien.ac.at

The approved original version of this diploma or master thesis is available at the main library of the Vienna University of Technology.
http://www.ub.tuwien.ac.at/eng

TECHNISCHE UNIVERSITÄT WIEN
Vienna University of Technology

begutachtet durch

Prof. Dr. Karsten Held

DIPLOMARBEIT

Vertex extensions of the dynamical mean field theory for the Falicov-Kimball model

Ausgeführt am Institut für Festkörperphysik
der Technischen Universität Wien

unter der Anleitung von

Prof. Dr. Karsten Held

Dr. Georg Rohringer

von

Tin Ribic

Matrikelnummer: 0925829
Anton-Baumgartnerstr. 44, 1230 Wien

WIEN, Januar 26, 2015

Tin Ribic

1 Deutsche Kurzfassung

Das Falicov-Kimball-Modell ist eines der einfachsten Modelle für Elektronen, das Phasenübergänge in Gittersystemen beschreibt. Es wurde eingeführt, um Metall-Halbleiter Übergänge theoretisch zu beschreiben [1]. Die Elektronen werden auf diskreten Gitterplätzen behandelt und in zwei Typen von Elektronen unterteilt, leichte, mobile Bandelektronen, oft auch als c-Elektronen bezeichnet und immobile f-Elektronen, welche stark an die Atomkerne des Gitters gebunden sind und daher nicht in der Lage sind, sich durch das System zu bewegen. Die Wechselwirkung zwischen den verschiedenen Arten von Elektronen wird im Modell in Form eines Wechselwirkungsparameters U behandelt, der die zusätzliche Energie angibt, die das System hat, wenn ein c und ein f-Elektron sich am selben Gitterplatz aufhalten. Der Hopping-Parameter t beschreibt die Mobilität der Bandelektronen. Dabei handelt es sich im Wesentlichen um die Übergangsamplitude für c-Elektronen zwischen benachbarten Gitterplätzen. Während das Verhalten der meisten wechselwirkenden quantenmechanischen Modelle entweder trivial oder extrem kompliziert ist, kann das Falicov-Kimball Modell teilweise analytisch behandelt werden, zeigt aber selbst dann noch eine nichttriviale Dynamik.

Das Ziel dieser Diplomarbeit war eine theoretische Behandlung des Falicov-Kimball Modells, welche über eine reine Molekularfeldnäherung hinausgeht. Dazu wurden auf Basis von Resultaten der dynamischen Molekularfeldtheorie Zweiteilchengrößen, sogenannte Vertexfunktionen, berechnet. Neben dem vollen Vertex, der die totale Streuamplitude zweier Elektronen beschreibt, konnte auch eine Zerlegung dieser Streuprozesse nach der topologischen Struktur vorgenommen werden, um irreduzible Vertices zu gewinnen. Diese wurden wiederum zur Berechnung von nicht-lokalen Suszeptibilitäten verwendet. Speziell die Ladungs-Ladungs Suszeptibilität beschreibt einen Phasenübergang des Systems von einer ungeordneten Phase in eine "Schachbrett"-Ordnung, bei der abwechselnd c- und f-Elektronen auf einem kubischen Gitter verteilt sind.

Zusätzlich wurde die one-particle-irreducible ($1PI$) Methode auf das Falicov-Kimball angewandt, um nichtlokale Korrelationen und Selbstenergien zu berechnen. Der Vorteil der Methode liegt, im Gegensatz zu anderen Erweiterungen der DMFT, in der kontrollierten Behandlung der Aufteilung zwischen lokaler und nichtlokaler Dynamik, so dass die Ergebnisse der dynamischen Molekularfeldtheorie als Basis für $1PI$ Rechnungen verwendet werden können. Es war möglich geschlossene Ausdrücke auch für die Vertices der $1PI$-Fermionen zu gewinnen und dadurch die Selbstenergiekorrekturen in der $1PI$-Theorie zu berechnen. Viele der Ergebnisse konnten ohne numerische Rechnungen, also auf rein anaylytischem Wege, gewonnen werden. Neben den Einsichten zum Falicov-Kimball-Modell können so auch die Eigenschaften der verwendeten Methoden besser verstanden werden.

Contents

1 Deutsche Kurzfassung **2**

2 Introduction **4**

3 The Falicov-Kimball model **5**
3.1 Perturbation theory in the case of small U 5
3.2 Derivation of the c-electron Green's function 8
3.3 Ordering of the non-interacting Falicov-Kimball model 9
3.3.1 Ordering in the one-dimensional system 11
3.3.2 Ordering in the two-dimensional system 12

4 Dynamical mean field theory **15**
4.1 Dynamical mean field theory and infinite dimensions 15
4.2 The Resonant Level Model 16
4.3 Calculation of one-particle objects 17
4.4 Calculation of two-particle objects 18
4.5 Projecting bath states out of the Hamilton operator 22
4.6 Numerical dynamical mean field theory results 23

5 Structure of the vertices in local approximation and derived quantities **26**
5.1 Asymptotic behaviour of the local vertices from the DMFT calculation 26
5.1.1 Full vertex F 26
5.1.2 Particle-particle irreducible vertex Γ_{pp} 27
5.1.3 Particle-hole irreducible vertex Γ_{ph} 28
5.1.4 Fully irreducible vertex Λ 29
5.2 Ladder approximations for the full momentum dependent vertex F 30
5.2.1 Particle-particle ladder 31
5.2.2 Particle-hole ladder 32
5.3 Susceptibilities 34
5.4 Numerical results 35

6 Path integral approaches **38**
6.1 Integrating out bath states from the action of the resonant level model 38
6.2 Transformation of the Falicov-Kimball action 39
6.3 One Particle Irreducible approach 40
6.3.1 Ladder approximation for the one particle irreducible approach 43
6.3.2 $1PI$ corrections for the self energy 46
6.3.3 Numerical results for the self-energy corrections 47

7 Conclusion **51**

2 Introduction

The Falicov-Kimball model is one of the simplest models for electron systems where correlation effects can be observed. It was first introduced by Falicov and Kimball [1] to describe semiconductor-metal transitions. The idea was to have two types of electrons, tightly bound ones and moveable band electrons. The Coulomb repulsion between the two different types of electrons is treated in the model, while there is no interaction between the band electrons; the Falicov-Kimball model can be treated as an effective one-particle model for the itinerant electrons. In contrast to the similar Hubbard model [2], the behaviour of the mobile electrons in the Falicov-Kimball model can be predicted qualitatively, which is a consequence of the simple one-particle structure. Anyhow, there are correlations between the two types of electrons, indirectly leading to correlations between band electrons just as well. Such correlation effects make an analytical or numerical treatment of this system very difficult, since static mean-field like methods, like Density Functional Theory cannot describe the relevant physics. In this respect, dynamical mean field theory (DMFT) is a big step forward for its capability of describing correlations which are purely local in space, yet not necessarily in time. DMFT achieves this feat by regarding an impurity site with the full local interaction, instead of the whole lattice. The effect of the lattice is included as a hopping-reservoir from where electrons can hop to the impurity site and back into the bath. Analytical results for applying Dynamical Mean Field Theory to the Falicov-Kimball model in infinite dimensions exist [3], but they cannot describe spatial correlations. The focus of this thesis was hence to extend the DMFT by including nonlocal correlations through diagrammatic techniques, based on local quantities extracted from the DMFT calculations. Examples for such methods are the dynamical vertex approximation ($D\Gamma A$), the Dual-Fermion theory (DF) and the one-particle irreducible approach ($1PI$). While DMFT assumes the locality of a one-particle object, the self-energy Σ, the $D\Gamma A$, DF and $1PI$ methods are based on two-particle vertices. Thus the approximation is made at a much deeper level, including purely local correlations between two electrons. In contrast to DMFT, which uses the same self-energy for all electrons when returning from the impurity problem to the lattice problem, the vertex-based methods include two-particle objects in their description of the lattice as well. Anyhow, even $D\Gamma A$ and similar approximations are not expected to describe the checkerboard-ordered phase of the Falicov Kimball model, which occurs at low temperatures [4], as the lattice is not homogeneous any more. To treat the model in this regime, the symmetry breaking has to be introduced manually into the calculation, necessitating either a symmetry-broken calculation or the use of cluster extensions of the impurity for the mean-field theory.

Since the Falicov-Kimball can be treated analytically in some respects, the obtained results are analytical as well, allowing for easier interpretation and comparison with numerical results for similar models, for example the Hubbard model. The thesis is organized as follows: First a discussion of general features of the Falicov-Kimball model will be given, before discussing the applicability and results of perturbation theory as well. Then, the results of DMFT calculations are presented, being used later on as basis for the calculation of vertices and derived quantities. Those vertices are employed for the calculation of physical susceptibilities and as building blocks for a one-particle-irreducible treatment of the Falicov-Kimball system. The obtained two-particle objects are also used for a $1PI$-treatment of the Falicov-Kimball model, a method which allows for a controlled inclusion of calculated local quantities into the description of the full lattice.

3 The Falicov-Kimball model

The Hamilton operator for the Falicov-Kimball model is as follows:

$$\mathcal{H}_{FC} = -t \sum_{\langle i,j \rangle} c_i^\dagger c_j + \varepsilon_f \sum_i f_i^\dagger f_i + U \sum_i f_i^\dagger f_i c_i^\dagger c_i - \mu \sum_i (f_i^\dagger f_i + c_i^\dagger c_i). \tag{1}$$

Where the sums over i are performed over all lattice sites and the indices $\langle i, j \rangle$ go over all pairs of nearest neighbours. The chemical potential μ is assumed to be equal for all electrons, but possible deviations can be absorbed into the value of ε_f. Nearest-neighbour hopping only is assumed, with the hopping amplitude t defining the bare dispersion relation. Extensions beyond nearest-neighbour hopping are possible without introducing further complications. The on-site energy for localized electrons is given by ϵ_f, while a possible on-site energy for band electrons can be absorbed in the chemical potential. The $c_i^{(\dagger)}$ and $f_i^{(\dagger)}$ operators are the creation and annihilation operators at the lattice site i for localized and itinerant electrons, respectively; U is the Coulomb interaction between them. The model was proposed by Falicov and Kimball in 1969 for a description of metal-insulator transitions. The system is much simpler to treat than the Hubbard model, as the c-electrons do not interact with each other and the f-electrons cannot move. For these reasons, exact eigenstates could, in principle, be calculated by distributing the f-electrons and then solving the effective one-particle problem for the itinerant electrons. An important consequence is that actual many-electron eigenstates can be written as a single Slater determinant. Thus, the Falicov-Kimball model is an example of a disorder model, not a fully interacting model.
While the construction of eigenstates is straightforward, a full diagonalization for a given lattice is not feasible. For a lattice with N distinct sites, there are 2^N distinct configurations of f electrons. For each of these configurations, the resulting $N \times N$ matrix for the c-electrons would have to be diagonalized to get all the eigenstates of the resulting Hamilton operator for the c-electrons. Those c-Eigenstates can have Eigenvalues in the ranges $0 \pm n_{nn} t$ and $U \pm n_{nn} t$ only, with n_{nn} being the number of nearest neighbours a lattice site has. Any way, some analytic results for the Falicov-Kimball model exist. In the limit of infinite dimensions, dynamical mean field theory was successfully applied, yielding Green's functions for both c and f electrons [3]. The System is known to condense into periodic configurations of f-electrons at low temperatures [5], specifically into checkerboard-ordering at half-filling and in two [4] or three dimensions (see 5.4). When U is very small, perturbation theory can be used to approximate the solutions for the Falicov-Kimball model. A perturbative treatment of 1-particle states and energies for small values of t breaks down at the choice of a basis to perform the perturbation theory in, as there are abundant degenerate eigenstates, at least away from half-filling, but can be performed for the self-energy [6]. Within the degenerate subspaces, the eigenstates for the U-only part of the Hamilton operator would have to be orthogonalized under the hopping part of the Hamilton operator, for the perturbation theory to have any meaningful results.

3.1 Perturbation theory in the case of small U

If U is assumed to be small compared to t, perturbation theory can be used to calculate the behaviour of the system. The $\vec{k}$-eigenstates are used as a starting point, as the kinetic part of the Hamilton operator is diagonal in this basis. For performing the perturbation theory calculations, k and j are used as symbols to denote vectors in the reciprocal and real space, respectively. In this section, i is not used as index for lattice sites since it is needed as imaginary unit. The

creation and annihilation operators in the k basis are defined as:

$$c_k^\dagger = \frac{1}{\sqrt{N}} \sum_j c_j^\dagger e^{ikj} \tag{2a}$$

$$c_k = \frac{1}{\sqrt{N}} \sum_j c_j e^{-ikj} \tag{2b}$$

With the summations being performed over all lattice sites, N being the total number of lattice sites and kj the inner product between k and j. Rewriting the Hamiltonian (1) into the new basis gives:

$$\mathcal{H}_{FC}^k = \sum_k (\varepsilon_k - \mu) c_k^\dagger c_k + \varepsilon_f \sum_j f_j^\dagger f_j + U \sum_{j,k,k'} \frac{1}{N} f_j^\dagger f_j c_k^\dagger c_{k'} e^{i(k'-k)j} - \mu \sum_j f_j^\dagger f_j. \tag{3}$$

Here, ϵ_k, the energy of k-eigenstates was introduced. In the case of nearest-neighbour-hopping only, ϵ_k is given by:

$$\epsilon_k = -2t \sum_{i=1}^{D} \cos(k_i). \tag{4}$$

If $f_j^\dagger f_j$ is considered to be just a position-dependent number n_j^f which can be either 0 or 1, depending on whether the site i is occupied by a f-electron, with no spatial correlations, it is possible to calculate expectation values for the energy corrections by applying perturbation theory on a single-electron level, as there is no interaction between the itinerant electrons. The first order energy correction becomes:

$$\varepsilon_k^{(1)} = \langle \langle 0_c | c_k U \sum_{j,k',k''} \frac{1}{N} n_j^f c_{k'}^\dagger c_{k''} e^{i(k''-k')j} c_k^\dagger | 0_c \rangle \rangle_f. \tag{5}$$

Here, $|0_c\rangle$ is the vacuum state with respect to the c-electrons. The influence of the f electrons is included in n_j^f and $\langle\rangle_f$, the mean value over all configurations of f-electrons. Explicit evaluation gives:

$$\varepsilon_k^{(1)} = U \langle \sum_j \frac{1}{N} n_j^f \rangle_f. \tag{6}$$

It is convenient to introduce the probability of an arbitrary lattice site being occupied by an f-electron as

$$p_1 = \langle \sum_j \frac{1}{N} n_j^f \rangle_f. \tag{7}$$

$\varepsilon_k^{(1)}$ can then be expressed as:

$$\varepsilon_k^{(1)} = U p_1 \tag{8}$$

To perform a second order perturbation theory calculation, it would be necessary to orthogonalize all degenerate states for a given energy under the perturbation part of the Hamilton operator. As the system size increases, the number of degenerate states becomes small compared to the total number of states. Hence, their relative importance for the energy corrections decreases. For this reason, the orthogonalization has been neglected, which is a good approximation for sufficiently large systems. The corrections become:

$$\varepsilon_k^{(2)} = \langle \sum_{k' \neq k} |\langle 0_c | c_k U \sum_{j,k'',k'''} \frac{1}{N} n_j^f c_{k'}^\dagger c_{k''} e^{i(k'''-k'')j} c_{k'}^\dagger | 0_c \rangle|^2 \frac{1}{\varepsilon_k - \varepsilon_{k'}} \rangle_f \tag{9}$$

$$\varepsilon_k^{(2)} = \langle \sum_{k' \neq k} |U \sum_j \frac{1}{N} n_j^f e^{i(k-k')j}|^2 \frac{1}{\varepsilon_k - \varepsilon_{k'}} \rangle_f \tag{10}$$

To evaluate $\langle\rangle_f$ acting on the sum, let us consider ${n_j^f}^2 = n_j^f$. This is obviously true since n_j^f is either 0 or 1. One can then write

$$\sum_j n_j^f := \sum_j {n_j^f}^2 \tag{11}$$

For the expectation value $\langle\rangle_f$ of the equation, by using eq. (7) to rewrite the left hand side and introducing the Fourier series representations for n_j^f:

$$n_k^f = \sum_j n_j^f e^{-ikj} \frac{1}{\sqrt{N}} \tag{12}$$

$$n_j^f = \sum_k n_k^f e^{ikj} \frac{1}{\sqrt{N}} \tag{13}$$

One arrives at:

$$p_1 N = \langle \sum_{j,k,k'} n_k^f n_{k'}^f e^{i(k+k')j} \frac{1}{N} \rangle_f \tag{14}$$

Performing the summation over j, one gets $\delta_{k,-k'} N$ from the oscillatory phase.

$$p_1 N = \langle \sum_k n_k^f n_{-k}^f \rangle_f \tag{15}$$

Since n_j^f is a real function, n_{-k}^f is the conjugate complex of n_k^f and $n_k^f n_{-k}^f = |n_k^f|^2$. Thus the expectation value of the sum of all $|n_k^f|^2$ is known. The second order energy corrections in perturbation theory contain a sum over all $|n_k^f|^2$, except for $k = 0$. While an approximation $\langle |n_k^f|^2 \rangle_f \approx p_1$ might seem tempting, when regarding equation (15) and considering there are N summands in the right hand side, not all values of $\langle |n_k^f|^2 \rangle_f$ are equal. Specifically, $|n_{k=0}^f|$ is different from the others. This is a consequence of n_j^f being either 0 or 1 and thus introducing a positive bias. Calculating $\langle |n_{k=0}^f|^2 \rangle_f$ gives:

$${n_{k=0}^f}^2 = \sum_{j,l} n_j^f n_l^f \frac{1}{N} \tag{16}$$

This sum can be decomposed into a part where $j = l$ and the rest.

$${n_{k=0}^f}^2 = \sum_j n_j^f n_j^f \frac{1}{N} + \sum_{j \neq l} n_j^f n_l^f \frac{1}{N} \tag{17}$$

The expectation value of ${n_{k=0}^f}^2$ can be calculated analytically, if the n_j^f are assumed to be independent of each other, which they are in the original eigenbasis when $U = 0$. The first summand can then be expressed using (7).

$$\langle {n_{k=0}^f}^2 \rangle_f = p_1 + \langle \sum_{j \neq l} n_j^f n_l^f \frac{1}{N} \rangle_f \tag{18}$$

For the second summand, there are N possible values for j and $N-1$ possible values for l for each j. The term in the sum becomes 1 only if $n_j^f = n_l^f = 1$, for which the probability is ${p_1}^2$.

$$\langle {n_{k=0}^f}^2 \rangle_f = p_1 + (N-1){p_1}^2 = N{p_1}^2 + p_1(1-p_1) \tag{19}$$

It is convenient to introduce $p_2 = 1 - p_1$, the probability of a given lattice site not being occupied by an f electron. Subtracting this term from eq. (15) yields

$$\langle \sum_{k \neq 0} n_k^f n_{-k}^f \rangle_f = Np_1 - N{p_1}^2 - p_1 p_2 = (N-1)p_1 p_2 \tag{20}$$

Thus each of the $N-1$ summands on the left side can be approximated as $p_1 p_2$ if the mean value over all possible configurations of f-electrons is taken. When inserted into eq. (10) one gets:

$$\varepsilon_k^{(2)} = U^2 p_1 p_2 \sum_{k' \neq k} \frac{1}{\varepsilon_k - \varepsilon_{k'}} \tag{21}$$

These results can be used to predict the behaviour of the real part of the self-energy Σ in the DMFT calculation when U is small, or equivalently, p_1 is small. They can also be applied if p_2 is small, which can be easily seen by replacing $f_i^\dagger f_i$ with $1 - f_i f_i^\dagger$ in the original Hamilton operator, in which case the perturbation theory starts from the system filled with stationary electrons where $\Sigma = U$. From the results of perturbation theory, Σ is expected to be $\approx p_1 U + p_1 p_2 U^2 f(\omega)$ to leading order in p_1 and U, with $f(\omega)$ being a function depending on the frequency ω. It is also evident, that for the particle-hole symmetric case, there are no real corrections in second order perturbation theory if $\varepsilon_k = 0$ as a counter-term with opposite sign exists for every term in the sum. Additionally, Energies that are situated at edges of the original band are pushed outwards: if $\varepsilon_k > \varepsilon_{k'}$, then all the summands are positive, while $\varepsilon_k < \varepsilon_{k'}$ leads to all terms being negative. This is consistent with a beginning separation of Hubbard bands.

3.2 Derivation of the c-electron Green's function

In this section, some analytic results for the one-particle Green's function of the c electrons is to be derived. We start from the definition of the one-particle imaginary-time Green's function for itinerant electrons:

$$G_{j,i}^c(\tau) = \langle (c_j(\tau)\ c_i^\dagger)\Theta(\tau) - (c_i^\dagger\ c_j(\tau))\Theta(-\tau) \rangle \tag{22}$$

Here, Θ is the step function and the brackets $\langle\rangle$ denote teh calculation of a (thermal) mean value, including, but not being restricted to $\langle\rangle_f$. This object describes the propagation of electrons through the system. The imaginary-time Green's function has the advantage of being anti-periodic in the variable τ with a anti-periodicity length of $1/\beta$. This causes only discrete frequencies to appear in its Fourier transform, the so-called fermionic Matsubara frequencies

$$\nu_n = (2n+1)\frac{\pi}{\beta} \tag{23}$$

Differentiation of the Green's function with respect to the imaginary time variable yields:

$$\frac{d}{d\tau} G_{j,i}^c(\tau) = \langle (\frac{d}{d\tau} c_j(\tau)\ c_i^\dagger)\Theta(\tau) - (c_i^\dagger\ \frac{d}{d\tau} c_j(\tau))\Theta(-\tau) + (c_j\ c_i^\dagger + c_i^\dagger\ c_j)\delta(\tau) \rangle, \tag{24}$$

the equation of motion for the one-particle Green's function. The imaginary time-derivative of $c_j(\tau)$ is $[c_j(\tau), \mathcal{H}]$, while $(c_j\ c_i^\dagger + c_i^\dagger\ c_j) = \delta_{i,j}$. The commutator $[c_j(\tau), \mathcal{H}]$ can be evaluated with

relative ease. The total expression for the derivative becomes:

$$\frac{d}{d\tau}G^c_{j,i}(\tau) = \langle(-t\sum_{\langle l\rangle} c_l(\tau) + Uf^\dagger_j(\tau)f_j(\tau)c_j(\tau) - \mu c_j(\tau))c^\dagger_i\Theta(\tau) - \\ c^\dagger_i(-t\sum_{\langle l\rangle} c_l(\tau) + Uf^\dagger_j(\tau)f_j(\tau)c_j(\tau) - \mu c_j(\tau))\Theta(-\tau) + \delta_{i,j}\delta(\tau)\rangle \quad (25)$$

Here, the sum over l includes all lattices sites which are neighbours to the site with index j. The equation can be expressed in terms of Green's functions:

$$\frac{d}{d\tau}G^c_{j,i}(\tau) = -t\sum_{\langle l\rangle} G^c_{l,i}(\tau) - \mu G^c_{j,i}(\tau) + UG^{fc}_{j,j,j,i}(\tau,\tau,\tau) + \delta_{i,j}\delta(\tau) \quad (26)$$

Where the (mixed) two-particle Green's function,

$$G^{fc}_{i,j,k,l}(\tau_1,\tau_2,\tau_3) = \langle f^\dagger_i(\tau_1)f_j(\tau_2)c^\dagger_k(\tau_3)c_l(\tau_4)\rangle, \quad (27)$$

has been introduced. This equation is considered once for the on-site Green's function with $i = j$, $G_{on-site}$, and once for a nearest-neighbour Green's function, G_{nn}, assuming that the mixed two-particle Green's function $G^{fc}_{j,j,j,i}(\tau,\tau,\tau)$ is just $p_1 \cdot G^c_{j,i}(\tau)$ when the thermal mean value is calculated. The discussion should provide a scaling law when going to infinite dimensions or, equivalently, numbers of nearest neighbours (also called coordination numbers).

$$\frac{d}{d\tau}G^c_{on-site}(\tau) = -t\sum_{\langle l\rangle} G^c_{nn}(\tau) - \mu G^c_{on-site}(\tau) + Up_1G^c_{on-site}(\tau) + \delta(\tau) \quad (28)$$

$$\frac{d}{d\tau}G^c_{nn}(\tau) = -t\sum_{\langle l'\rangle} G^c_{nnn}(\tau) - tG^c_{on-site}(\tau) - \mu G^c_{nn}(\tau) + Up_1G^c_{nn}(\tau) \quad (29)$$

Now, the summation over l' includes all the neighbours to the lattice site j, apart from i, thus including next-nearest-neighbour (nnn) sites, with according Green's functions, G_{nnn}, to i and i itself. The summand which results in a on-site Green's function is treated separately. For $G_{on-site}$ to have an effect on the time evolution in eq. (29), without dominating it completely, $t\,G_{on-site}$ has to be of the order of magnitude of $(\mu - p_1U)G_{nn}$. If $\mu - U$ is assumed to be of order 1, G_{nn} has to be $\sim tG_{on-site}$. Knowing this and regarding eq. (28), there are N_{nn},with N_{nn} being the coordination number, nearest-neighbour Green's functions, which are added for the time evolution of $G_{on-site}$. Then $N_{nn}tG_{nn}$ has to be of the order of magnitude of $G_{on-site}$. From this, one can see that t^2N_{nn} has to be of the order of 1, which provides the scaling of t with N_{nn}.

$$t_{N_{nn}} = \frac{t_0}{\sqrt{N_{nn}}} \quad (30)$$

The hopping amplitude has to be scaled with the number of neighbours to make sure results with different numbers of neighbours are comparable [7]. $t_{N_{nn}}$ is the hopping amplitude when there are N_{nn} nearest neighbours, with t_0 being a constant.

3.3 Ordering of the non-interacting Falicov-Kimball model

Due to the antisymmetric nature of fermionic wave functions, the Pauli exclusion principle, fermionic systems show non-vanishing correlations even when they are non-interacting (bosonic systems also show correlations, even tough they are symmetric instead of antisymmetric). These correlations are usually called exchange correlations and not considered to be "true correlations".

In the following, the explicit expressions for the charge-charge correlation function for c-electrons at zero temperature and half-filling are calculated for the one- and two-dimensional Falicov-Kimball model. This shows that the tendency of the Falicov-Kimball model for checkerboard-ordering is an effect of the band-structure. While the repulsion between c- and f-electrons drives the system towards localization and ordering, the band structure accounts for the specific choice of ordering. The object that needs to be investigated is the charge-charge correlation function,

$$\chi_{CC}(\Delta) = \langle c_j^\dagger c_j c_{j+\Delta}^\dagger c_{j+\Delta}\rangle - \langle c_j^\dagger c_j\rangle\langle c_{j+\Delta}^\dagger c_{j+\Delta}\rangle, \tag{31}$$

where $c_j^{(\dagger)}$ are again the creation and annihilation operators for band electrons at the site labelled j, Δ is a distance between two sites here and $\langle\rangle$ denotes the calculation of an expectation value. So far, no assumptions on the dimensionality of the problem were made. Since the model shows translational invariance, the correlation function was assumed to depend on the distance between the two sites only and not on their explicit positions. It is now possible to write the creation and annihilation operators in terms of Fourier-transformed creation and annihilation operators, using the relations (see also eq (2))

$$c_j^\dagger = \frac{1}{\sqrt{N}}\sum_k e^{-ikj} c_k^\dagger \tag{32a}$$

$$c_j = \frac{1}{\sqrt{N}}\sum_k e^{ikj} c_k. \tag{32b}$$

χ_{CC} then takes the form

$$\chi_{CC}(\Delta) = \frac{1}{N^2}\langle \sum_{k_1,k_2,k_3,k_4} e^{i(k_4-k_3+k_2-k_1)j} e^{i(k_4-k_3)\Delta} c_{k_1}^\dagger c_{k_2} c_{k_3}^\dagger c_{k_4}\rangle - \frac{1}{N^2}\langle \sum_{k_1,k_2} e^{i(k_2-k_1)j} c_{k_1}^\dagger c_{k_2}\rangle\langle \sum_{k_1,k_2} e^{i(k_2-k_1)(j+\Delta)} c_{k_1}^\dagger c_{k_2}\rangle. \tag{33}$$

At zero temperature, the occupation of each state is known to be 0 if the states energy is larger than the chemical potential and 1 if it is smaller. This allows for an easy calculation of the correlation function by Wick's theorem. For the two expectation values containing only one creation and annihilation operator each, this is trivial, yielding

$$\langle c_{k_1}^\dagger c_{k_2}\rangle = \delta_{k_1,k_2}\Theta(-\epsilon_{k_1}). \tag{34}$$

Here, δ is the Kronecker-delta, Θ is the step-function and ϵ_k being the k-dependent band-electron energy. The chemical potential is zero at the desired half-filling. For the term containing four creation and annihilation operators, more than one pairing is possible. In total, two cases have to be considered:

$$\langle c_{k_1}^\dagger c_{k_2} c_{k_3}^\dagger c_{k_4}\rangle = \delta_{k_1,k_2}\Theta(-\epsilon_{k_1})\delta_{k_3,k_4}\Theta(-\epsilon_{k_3}) + \delta_{k_1,k_4}\Theta(-\epsilon_{k_1})\delta_{k_3,k_2}\Theta(+\epsilon_{k_3}) \tag{35}$$

Note the sign in the step function for the exchange term, originating from the ordering of the operators. Inserting these expressions into the original expression for χ_{CC} yields:

$$\chi_{CC}(\Delta) = \frac{1}{N^2}\sum_{k_1,k_3}\Theta(-\epsilon_{k_1})\Theta(-\epsilon_{k_3}) + \frac{1}{N^2}\sum_{k_1,k_3} e^{i(k_1-k_3)\Delta}\Theta(-\epsilon_{k_1})\Theta(+\epsilon_{k_3}) - \frac{1}{N^2}\sum_{k_1}\Theta(-\epsilon_{k_1})\sum_{k_1}\Theta(-\epsilon_{k_1}) \tag{36}$$

Since the first sum factorizes and is, up to a sign, equal to the last one, they cancel each other. Hence, only the term

$$\frac{1}{N^2}\sum_{k_1,k_3} e^{i(k_1-k_3)\Delta}\Theta(-\epsilon_{k_1})\Theta(+\epsilon_{k_3}) \tag{37}$$

has to be considered. The cancelling and vanishing due to scaling are not specific to the choice of dispersion relation and chemical potential, but hold for general non-interacting fermionic systems. The remaining term will be calculated analytically in 1 and 2 dimensions. While functions, which have their Fourier transform's amplitudes clustered around 0 are expected to "cluster", in the sense that if the amplitude of the function at a certain position in real space is known, that the (real-space) amplitudes in the region are expected to be similar, the sign in the fermionic exchange term actually pushes other electrons away, even more than might be expected by Pauli's principle alone.

3.3.1 Ordering in the one-dimensional system

The charge-charge correlation function in one dimension is easily calculated if the summation in

$$\frac{1}{N^2}\sum_{k_1,k_3} e^{i(k_1-k_3)\Delta}\Theta(-\epsilon_{k_1})\Theta(+\epsilon_{k_3}) \tag{38}$$

is replaced by an integration, thus yielding

$$\frac{1}{N^2}\int dk_1 dk_3 \frac{N^2}{(2\pi)^2} e^{i(k_1-k_3)\Delta}\Theta(-\epsilon_{k_1})\Theta(+\epsilon_{k_3}). \tag{39}$$

If we consider a dispersion relation where the k-states between $\pm\pi/2$ are filled at zero temperature, $\Theta(-\epsilon_k)$ restricts the integration to the area where $|k| < \frac{\pi}{2}$ or $|k| > \frac{\pi}{2}$ for k_1 and k_2 respectively, resulting in the expression

$$\chi_{CC}^{1D}(\Delta) = \frac{1}{(2\pi)^2}\left(\int_{-\pi/2}^{\pi/2} dk_1 e^{ik_1\Delta}\right)\left(\int_{\pi/2}^{3\pi/2} dk_3 e^{-ik_3\Delta}\right) \tag{40}$$

$$\chi_{CC}^{1D}(\Delta) = \left(\frac{\sin(\Delta\pi/2)}{\Delta\pi}\right)^2 (-1)^{\Delta} \tag{41}$$

One might argue that the factor $(-1)^{\Delta}$ can be replaced by -1 since $\sin(\Delta\pi/2)$ only contributes for uneven values of Δ. This is correct everywhere, except when the limes $\Delta \to 0$ is taken and the correlation function suddenly becomes positive. The result implies that an electron displaces nearest neighbouring electrons, third-nearest neighbouring electrons and other uneven-numbered-nearest-neighboured electrons, but does not affect even-numbered ones, since $\sin(\Delta\pi/2)$ becomes 0 for even values of Δ. χ_{CC} is also associated with the exchange-hole induced by any given electron. The exchange hole gives the difference between the probability of finding an electron at a position and finding an electron at the same position, under the assumption that another electron is found at a given relative position. Up to a factor $1/2$, χ_{CC} and the exchange hole are equal for all values of $\Delta \neq 0$. χ_{CC} is smaller by a factor $1/2$ because it does not assume a-priori that an electron is found and for half-filling the probability of finding an electron at any site is $1/2$. The value of the exchange hole is $-1/2$ for $\Delta = 0$ as two electrons cannot occupy the same state. When performing a summation over the exchange hole over all sites in the limit of a large system:

$$\sum_{\Delta\neq 0} -2\left(\frac{\sin(\Delta\pi/2)}{\Delta\pi}\right)^2 - \frac{1}{2} = -4\frac{1}{\pi^2}\sum_{n=0}^{\infty}\frac{1}{(2n+1)^2} - \frac{1}{2} = -1, \tag{42}$$

the total electron-deficit in the rest of the system becomes 1. Below, the influence on the electron density caused by the exchange hole is plotted.

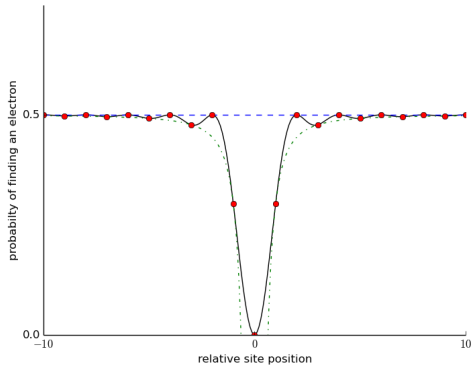

Figure 1: effect of the exchange hole on the probability of finding an electron

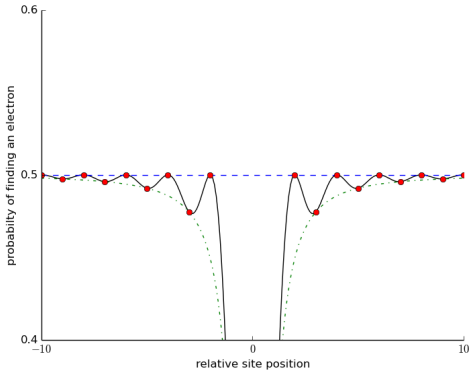

Figure 2: enlarged version of figure 1, showing unaffected sites

In figure 1 and 2, one can see how a localized electron displaces other ones. The dashed line gives the unperturbed probability of finding an electron at any site, i.e. 1/2. The full line shows the behaviour of the exchange-hole function, including non-integer values of Δ. The chain-dotted line is a representation of the auxiliary probability function $F_{aux}(\Delta)$,

$$F_{aux}(\Delta) = \frac{1}{2} - \frac{1}{(\pi\Delta)^2}, \tag{43}$$

which gives the same probability as the exchange hole for finding an electron at uneven-numbered neighbours. The dots emphasize the values of the probability for integer values of Δ, where lattice sites are located.

3.3.2 Ordering in the two-dimensional system

For the two-dimensional system, the non-interacting correlation function is calculated similarly to the one dimensional case. The k-summation is again replaced by an integral,

$$\frac{1}{N^2}\int d^2k_1 d^2k_3 \frac{N^2}{(2\pi)^4} e^{i(k_1-k_3)\Delta}\Theta(-\epsilon_{k_1})\Theta(+\epsilon_{k_3}), \tag{44}$$

where k_1, k_3 and Δ are now vectors. The integrals over k_1 and k_3 now factorize and will be investigated in the following. First the k_1-integration is considered:

$$\int d^2k_1 e^{ik_1\Delta}\Theta(-\epsilon_{k_1}) \tag{45}$$

The Fermi-surface, actually Fermi-line, of a half-filled, nearest-neighbour-hopping model in two dimensions is a square whose corners lie on the centres of the edges of the Brillouin-zone, as seen in figure 3.

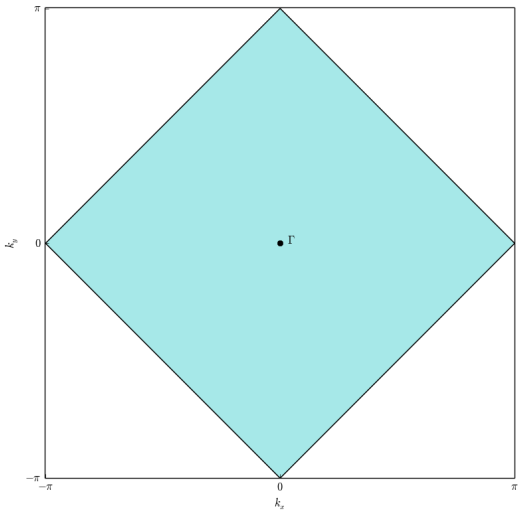

Figure 3: The filled region in the Brillouin zone for a two dimensional system with nearest neighbour Hopping on a square lattice at half-filling

The integration is now explicitly written as

$$\int_{-\pi}^{0} dk_x e^{ik_x\Delta_x} \int_{-k_x-\pi}^{\pi+k_x} dk_y e^{ik_y\Delta_y} + \int_{0}^{\pi} dk_x e^{ik_x\Delta_x} \int_{k_x-\pi}^{\pi-k_x} dk_y e^{ik_y\Delta_y}, \tag{46}$$

where k and Δ have been split into their components. One can see that for each point (k_x, k_y) included in the first integral in the above expression, $(-k_x, -k_y)$ is included in the second. This is equivalent to a complex conjugation of the integrand $\exp(i(k_x\Delta_x + k_y\Delta_y))$. Thus, two times the real part of one integral equals the sum of both of them. For this reason, only the second integral is evaluated, yielding:

$$2\frac{\cos(\Delta_y\pi) - \cos(\Delta_x\pi)}{\Delta_x^2 - \Delta_y^2}, \tag{47}$$

if only the real part is considered. It has to be multiplied with another factor 2, as twice the real part is needed as solution to equation (45). Now, the second integral in equation (44) needs to be evaluated.

$$\int d^2k_3 e^{-ik_3\Delta}\Theta(+\epsilon_{k_3}) \tag{48}$$

can be transformed by a shift of $k_3 \to k_3 + \Pi$, with Π being defined as (π, π). The integral then reads

$$e^{-i\Pi\Delta} \int d^2k_3 e^{-ik_3\Delta}\Theta(-\epsilon_{k_3}). \tag{49}$$

This is the factor $e^{-i\Pi\Delta}$ times the complex conjugate of equation (45), which has in turn already been established as real and being solved by (47) times 2. The total correlation function is then given by

$$\chi_{CC}^{2D}(\Delta_x, \Delta_y) = \left(\frac{\cos(\Delta_y\pi) - \cos(\Delta_x\pi)}{(\Delta_x^2 - \Delta_y^2)\pi^2}\right)^2 e^{i\pi(\Delta_x+\Delta_y)}. \tag{50}$$

The factor $\exp(i\pi(\Delta_x + \Delta_y))$ is always -1 when the other term is non-zero as either Δ_x or Δ_y needs to be even while the other one is odd for the difference of the $\cos(\Delta_x\pi)$ and $\cos(\Delta_y\pi)$ to be non-zero, making their sum odd and $\exp^{\pi(\Delta_x+\Delta_y)} = -1$. The exception to this behaviour

occurs in the limes $\Delta \to (0,0)$, where χ^{2D}_{CC} again goes to 1/4. The case $\Delta_x = \Delta_y$ needs to be treated separately, but the correlation function can be shown to converge towards

$$\chi^{2D}_{CC}(\Delta_x = \Delta_y) = \left(\frac{\sin(\Delta_x \pi)}{2\Delta_x \pi}\right)^2 e^{i2\Delta_x \pi}, \tag{51}$$

which is zero for all integer values of Δ_x, except when $\Delta_x = \Delta_y = 0$, where it goes to 1/4. With the correlation function known, the probabilities of finding an electron at a site, given that another on is located at a known relative position has been calculated.

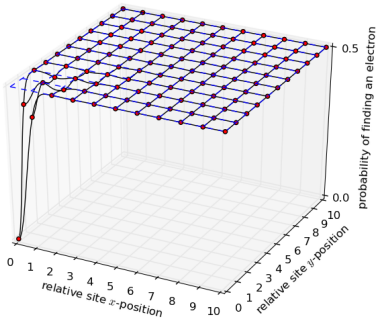

Figure 4: effect of the exchange hole on the probability of finding an electron

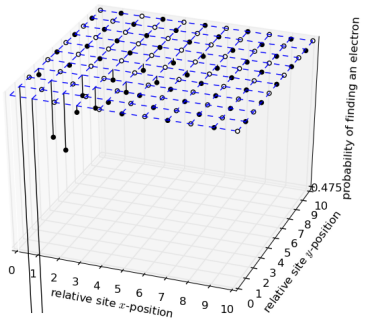

Figure 5: enlarged version of figure 4, showing unaffected sites

The probabilities where plotted in a similar fashion to the one-dimensional case, but for the detailed view, the continuation of the probability for non-integer values was omitted. Instead, the points where coloured black and white for affected and non-affected sites, respectively. The points associated with affected sites are connected to the plane of undisturbed probability by a line.

4 Dynamical mean field theory

While a solution for the finite-dimensional Falicov-Kimball model can not be obtained analytically, it can be treated exactly when the coordination number goes to infinity [3] [8]. When going to infinite dimension, it is necessary to scale the hopping parameter t with a factor $1/\sqrt{N}$, with N being the new coordination number, to avoid a trivial limit where one of the terms in the Hamilton operator can be neglected completely. In principle, U and μ could equivalently be scaled with the inverse of the factor, but this approach is less intuitive and leads to all terms diverging. Why this scaling is necessary can be seen from eqs. (25) to (29). A full diagonalization of the Hamiltonian for an interacting system with more than just a few particles is not feasible. Approximative methods, such as density functional theory (DFT) (which only gives mean-field like results, but allows for reliable calculations in weakly correlated materials) and dynamical mean field theory (DMFT), have been developed to be able to treat such problems. Here, a DMFT approach to the Falicov-Kimball model will be presented, as this model allows for the calculation of correlations in time (albeit not in space). The idea of replacing the finite-dimensional non-local problem by an infinite-dimensional local one was described in [9]. DMFT has become a well accepted theory for description of site-local electronic correlations.

4.1 Dynamical mean field theory and infinite dimensions

It has already been established that a straightforward diagonalization of the Falicov-Kimball Hamiltonian is not feasible for systems of a reasonable size. Since interesting phenomena occur when the kinetic and interaction term in the Hamiltonian are of similar size, there is no small parameter to build a perturbation theory on, either. Dynamical mean field theory offers the means of treating such systems. The basic premise of mean field theories is to treat most of the system as a bath, in which a single site is investigated more closely. The bath is treated as non-interacting, but coupled to the site in question and it has to behave consistently with the closely investigated site.
For the Falicov-Kimball model, such an approach may not seem applicable as a single site will either be occupied by an f-electron or not, and depending on this it will show completely different features. Indeed, DMFT fails at describing microscopic quantities for the Falicov-Kimball model and is only applicable if one is interested in spatial mean values. In this section, the assumptions DMFT builds on for the Falicov-Kimball model will be discussed, along with the limitations this causes for the extracted results.
Considering a system described by the Falicov-Kimball model, there certainly is a probability of finding an f-electron at a site, called p_1. If one assumes that the system is homogeneous and that the f-electrons are distributed randomly, any site has a chance p_1 of being occupied and $p_2 = 1 - p_1$ of being unoccupied by an f-electron. One can now investigate two sites, an occupied and an unoccupied one. If the system is large and disordered enough, their baths should be similar. As the rest of the system consists of a mix of occupied and unoccupied sites, it should not be consistent with neither the occupied nor the unoccupied one, instead being consistent with a weighted average of them.
As a next step, the role of the "bath" and the term "consistent" have to be defined. The bath should mimic the effects the rest of the system has on a single site, it should allow for transport of c-electron amplitudes. In principle, the Hamiltonian of the remaining system could be diagonalized and the eigenstates calculated. When the site is then connected to the bath again, those states have to hybridize with the localized state at the site, leading to a term

$$\sum_l ((\epsilon_l - \mu) c_l^\dagger c_l - t_l c_l^\dagger c_i - t_l^* c_i^\dagger c_l) \tag{52}$$

in the Hamiltonian describing the site coupled to the bath. l labels the bath-states, ϵ_l are the bath-energies, t_l is the hybridization between the bath state l and the localized electron state at the site i. $c_l^{(\dagger)}$ are operators associated with the creation and annihilation of bath states and $c_i^{(\dagger)}$ are the operators for the localized state.
Defining "consistency" is trickier. For the exemplary system described by a mean field theory, an Ising spin-system, the choice is clear, as the only interesting variable in the system is the magnetization and the mean bath-magnetization can be equalled to the expectation value of the local one, thus giving an obvious self-consistency condition. Most of the interesting expectation values of the Falicov-Kimball model can be expressed in terms of Green's functions, so they are a natural choice as a consistent variable. The local model can obviously only be used to calculate local Green's functions, containing information about local interactions, while the bath has to simulate the effects of the remaining lattice, thus carrying the information about the kinetic part of the Hamiltonian. However, this separation is not strict, it only gives an idea about which part of the calculation has to become trivial when either the interaction or the kinetic energy part in the Hamiltonian vanish-if t is zero, there is no hybridization and the bath has no effect on the site, if there is no interaction, the self-energy is identically 0 and one recovers the non-interacting dispersion relation for the system. In practice, the purely local self-energy, Σ [8] is extracted from the impurity problem. Then the local Green's function is calculated from the dispersion relation of the lattice in question and the local Green's function, updating the bath for the impurity.

4.2 The Resonant Level Model

In DMFT the full lattice is within DMFT approximated by a single site [3] [10], embedded in a non-interacting bath of one-particle states. For the Falikov-Kimball model, the corresponding Hamilton operator is of the form of a resonant level model:

$$\mathcal{H}_{RLM} = \varepsilon_f f_i^\dagger f_i + U f_i^\dagger f_i c_i^\dagger c_i - \mu(f_i^\dagger f_i + c_i^\dagger c_i) + \sum_l ((\epsilon_l - \mu) c_l^\dagger c_l - t_l c_l^\dagger c_i - t_l^* c_i^\dagger c_l) \tag{53}$$

Where i denotes the interacting lattice site one is currently interested in, and the summation over l including all the bath states. t_l is the hybridization between the on-site and the bath states and is related to the hopping parameter t. It is possible to choose all t_l to be real by adjusting the phase of the state associated with $c_l^\dagger$. A calculation of the imaginary time derivative of the on-site Green's function, called $G_{RLM}(\tau)$,

$$G_{RLM}^c(\tau) = \langle (c_i(\tau)\ c_i^\dagger)\Theta(\tau) - (c_i^\dagger\ c_i(\tau))\Theta(-\tau)\rangle, \tag{54}$$

yields:

$$\begin{aligned}\frac{d}{d\tau}G_{RLM}(\tau) = \langle (\sum_l -t_l^* c_l(\tau) + U f_i^\dagger(\tau) f_i(\tau) c_i(\tau) - \mu c_i(\tau)) c_i^\dagger \Theta(\tau) \\ - c_i^\dagger (\sum_l -t_l^* c_l(\tau) + U f_i^\dagger(\tau) f_i(\tau) c_i(\tau) - \mu c_i(\tau))\Theta(-\tau) + \delta(\tau)\rangle\end{aligned} \tag{55}$$

upon introducing the mixed c-f 2-particle Green's function,

$$G_{fc,i,i}^2(\tau,\tau,\tau) = \langle f_i^\dagger(\tau) f_i(\tau) c_i(\tau) c_i \Theta(\tau) - c_i f_i^\dagger(\tau) f_i(\tau) c_i(\tau)\Theta(-\tau)\rangle, \tag{56}$$

one can rewrite equation (56).

$$\frac{d}{d\tau}G_{RLM}(\tau) = \sum_l -t_l^* G_{l,i}(\tau) + U G_{fc,i,i}^2(\tau,\tau,\tau) - \mu G_{RLM}(\tau) + \delta(\tau) \tag{57}$$

$G^2_{fc,i,i}(\tau,\tau,\tau)$ is either $G_{RLM}(\tau)$ or 0, depending on the whether $f_i^\dagger(\tau)f_i(\tau)$ is 1 or 0, which is a conserved quantity. To get rid of the off-diagonal Green's function $G_{l,i}(\tau)$ in this expression, one can calculate its imaginary time derivative and transform the resulting and the original equation into Fourier series.

$$\frac{d}{d\tau}G_{l,i}(\tau) = -t_l G_{RLM}(\tau) + (\epsilon_l - \mu)G_{l,i}(\tau) \tag{58}$$

$$i\nu\, G_{l,i}(\nu) = -t_l G_{RLM}(\nu) + (\epsilon_l - \mu)G_{l,i}(\nu) \tag{59}$$

$$i\nu\, G_{RLM}(\nu) = \sum_l -t_l^* G_{l,i}(\nu) + U(0 \vee 1)G_{RLM}(\nu) - \mu G_{RLM}(\nu) + 1 \tag{60}$$

Now, eq. (59) allows for $G_{l,i}(\nu)$ to be eliminated from eq. (60). The total expression for $G_{RLM}(\nu)$ then becomes

$$G_{RLM}(\nu) = \sum_l \frac{t_l^*\, t_l}{i\nu - \epsilon_l + \mu} G_{RLM} + U(0 \vee 1)G_{RLM}(\nu) - \mu G_{RLM}(\nu) + 1 \tag{61}$$

The sum $\sum_l \frac{t_l^*\, t_l}{i\nu - \epsilon_l + \mu}$ is called the hybridization function $\Delta(\nu)$.

$$\Delta(\nu) = \sum_l \frac{t_l^*\, t_l}{i\nu - \epsilon_l + \mu}. \tag{62}$$

Introducing Δ, one can write:

$$G_{RLM}(\nu) = \frac{1}{i\nu - \Delta(\nu) - U(0 \vee 1) + \mu}. \tag{63}$$

4.3 Calculation of one-particle objects

With the Green's function from eq (63) as starting point, the full Green's function and self-energy can be calculated. If p_1 is the average f-electron occupation, the local Green's function can be written as:

$$G(\nu) = \langle G_{RLM}(\nu)\rangle = p_1 \frac{1}{i\nu - \Delta(\nu) - U + \mu} + (1 - p_1)\frac{1}{i\nu - \Delta(\nu) + \mu}. \tag{64}$$

To avoid lengthy expressions, the two parts are called:

$$\underset{\sim}{G}(\nu) = \frac{1}{i\nu - \Delta(\nu) + \mu}, \tag{65a}$$

$$\widetilde{G}(\nu) = \frac{1}{i\nu - \Delta(\nu) - U + \mu}. \tag{65b}$$

These are the one-particle Green's functions depending on the f-occupation at the site (0 or 1). To extract the self-energy, the Dyson equation can be used.

$$G_0^{-1}(\nu) = G^{-1}(\nu) + \Sigma(\nu) \tag{66}$$

In this context, G_0 is $\underset{\sim}{G}$, the Green's function for $U = 0$. Inserting for G and $\underset{\sim}{G}$ yields:

$$\Sigma(\nu) = p_1 U \frac{1}{1 - p_2\, \underset{\sim}{G}(\nu)U}. \tag{67}$$

Also, the following useful expressions can be derived:

$$\widetilde{G}(\nu) = \frac{G(\nu)\Sigma(\nu)}{p_1 U}, \tag{68a}$$

$$\underset{\sim}{G}(\nu) = \frac{G(\nu)\,(U - \Sigma(\nu))}{p_2 U}, \tag{68b}$$

$$G(\nu)\,(U - \Sigma(\nu))\,\Sigma(\nu) = -(p_1 U - \Sigma(\nu)). \tag{68c}$$

4.4 Calculation of two-particle objects

Let us turn our attention to the two-particle Green's functions which are needed to calculate the desired vertex functions. Wick's theorem [11] allows for calculating the two-particle Green's function G^2 for the c-electrons,

$$G^2(\tau'', \tau', \tau) = \langle \mathbf{T} c_i^\dagger(\tau'') c_i^\dagger(\tau') c(\tau) c \rangle \tag{69}$$

for non-interacting systems from a given one-particle Green's function. Here, the Fourier transform to frequency space of Wick's theorem is expressed in particle-hole notation.

$$G^2(\nu, \nu', \omega) = \beta G(\nu) G(\nu' + \omega)(\delta_{\omega,0} - \delta_{\nu,\nu'}) \tag{70}$$

To apply Wick's theorem to the Falicov-Kimball model in infinite dimensions, one must treat the case of presence and absence of f-electrons separately, adding them up with weights p_1 and p_2 respectively.

$$G^2_{FC}(\nu, \nu', \omega) = \beta(p_1 \widetilde{G}(\nu)\widetilde{G}(\nu' + \omega) + p_2 \underset{\sim}{G}(\nu)\underset{\sim}{G}(\nu' + \omega))(\delta_{\omega,0} - \delta_{\nu,\nu'}) \tag{71}$$

At this point in the calculation, correlation effects arise. With G^2_{FC}, which is called just G^2 from here on, available, one can now proceed to calculate the full vertex F, the vertices Γ_ν, irreducible in the channels $\nu = ph$, $\overline{ph}$ and pp as well as the fully irreducible vertex Λ. The full vertex is easily obtained from:

$$G^2(\nu, \nu', \omega) = \beta G(\nu) G(\nu' + \omega)(\delta_{\omega,0} - \delta_{\nu,\nu'}) + G(\nu) G(\nu + \omega) F^{\nu\nu'\omega} G(\nu') G(\nu' + \omega) \tag{72}$$

when inserting the known quantities G^2 and $G(\nu)$. After a lengthy evaluation it can be written as

$$F^{\nu\nu'\omega} = \beta(\delta_{\omega,0} - \delta_{\nu,\nu'}) \frac{(\Sigma(\nu) - U)\Sigma(\nu)(\Sigma(\nu' + \omega) - U)\Sigma(\nu' + \omega)}{p_1 p_2 U^2} \tag{73}$$

or, equivalently

$$F^{\nu\nu'\omega} = \beta(\delta_{\omega,0} - \delta_{\nu,\nu'}) \frac{(\Sigma(\nu) - p_1 U)(\Sigma(\nu' + \omega) - p_1 U)}{G(\nu) G(\nu' + \omega) p_1 p_2 U^2}. \tag{74}$$

The next step is to calculate the irreducible vertices in the pp, ph and $\overline{ph}$ channels by inserting F in the appropriate Bethe-Salpeter equations. Starting with the particle-particle irreducible vertex Γ_{pp}, this will be elaborated on in the following. For the calculation of Γ_{pp} it is advantageous to adopt particle-particle notation. To get F's representation in particle-particle notation, one has to replace all references to ω with $\overline{\omega} - \nu - \nu'$. In the following, we will relabel $\overbrace{\omega} \to \omega$. The corresponding Bethe-Salpeter equation [12] can be written as

$$F_{pp}^{\nu\nu'\omega} = \Gamma_{pp}^{\nu\nu'\omega} + \frac{1}{2\beta} \sum_{\nu_1} F_{pp}^{\nu(\omega-\nu_1)\omega} G(\nu_1) G(\omega - \nu_1) \Gamma_{pp}^{\nu_1\nu'\omega} \tag{75}$$

in particle-particle notation. $F_{pp}^{\nu\nu'\omega}$ is proportional to $(\delta_{\omega-\nu-\nu',0} - \delta_{\nu,\nu'})$, so that for a given value of ω it only has non-zero entries in the main diagonal and one skew diagonal. When regarding eq. (75) as a matrix equation in the indices ν and ν', one can see that Γ_{pp} has to inherit this structure from F. Thus, with an Ansatz

$$\Gamma_{pp}^{\nu\nu'\omega} = (\delta_{\omega-\nu-\nu',0} - \delta_{\nu,\nu'}) \tilde{\Gamma}^{\nu\nu'\omega} \tag{76}$$

it is possible to solve eq. (75) for $\tilde{\Gamma}$ by applying the crossing symmetry relations

$$\Gamma_{pp}^{\nu\nu'\omega} = -\Gamma_{pp}^{\nu(\omega-\nu')\omega} \tag{77}$$

and

$$F_{pp}^{\nu\nu'\omega} = -F_{pp}^{\nu(\omega-\nu')\omega}. \tag{78}$$

Upon inserting the Ansatz, there are two differences of Kronecker-deltas in the sum, which have to be multiplied with each other. This yields 4 terms, of which 2 are equivalent and can be summed up when considering the crossing symmetry. Finally, Γ_{pp} becomes

$$\Gamma_{pp}^{\nu\nu'\omega} = \beta(\delta_{\omega-\nu-\nu',0} - \delta_{\nu,\nu'})\frac{(\Sigma(\nu)-U)\Sigma(\nu)(\Sigma(\omega-\nu)-U)\Sigma(\omega-\nu)}{p_1p_2U^2 + (\Sigma(\nu)-p_1U)(\Sigma(\omega-\nu)-p_1U)} \tag{79}$$

in particle-particle, and

$$\Gamma_{pp}^{\nu\nu'\omega} = \beta(\delta_{\omega,0} - \delta_{\nu,\nu'})\frac{(\Sigma(\nu)-U)\Sigma(\nu)(\Sigma(\nu'+\omega)-U)\Sigma(\nu'+\omega)}{p_1p_2U^2 + (\Sigma(\nu)-p_1U)(\Sigma(\nu'+\omega)-p_1U)} \tag{80}$$

in particle-hole notation.
Let us now turn to the particle-hole and transverse particle-hole channel. These do not need to be treated separately, as they are related via the crossing relation

$$\Gamma_{\overline{ph}}^{\nu\nu'\omega} = -\Gamma_{ph}^{\nu(\nu+\omega)(\nu'-\nu)}. \tag{81}$$

Thus, only $\Gamma_{ph}^{\nu\nu'\omega}$ is derived explicitly. The corresponding Bethe-Salpeter equation, expressed in particle-hole notation, reads:

$$F^{\nu\nu'\omega} = \Gamma_{ph}^{\nu\nu'\omega} - \frac{1}{\beta}\sum_{\nu_1}\Gamma_{ph}^{\nu\nu_1\omega}G(\nu_1)G(\nu_1+\omega)F^{\nu_1\nu'\omega} \tag{82}$$

As $F^{\nu\nu'\omega} \sim (\delta_{\omega,0} - \delta_{\nu,\nu'})$, it is a diagonal matrix in ν and ν' for the case $\omega \neq 0$ and the equation above is easily solved. Γ then becomes a diagonal matrix as well and can be written as:

$$\Gamma_{ph}^{\nu\nu'\omega\neq 0} = \frac{F^{\nu\nu'\omega}}{1 - \frac{1}{\beta}G(\nu)G(\nu'+\omega)F^{\nu\nu'\omega}} \tag{83}$$

Note that the summation over ν_1 has already been performed and it has been replaced either by ν or ν'. Explicit evaluation gives:

$$\Gamma_{ph}^{\nu\nu'\omega\neq 0} = -\beta\delta_{\nu,\nu'}\frac{(\Sigma(\nu)-U)\Sigma(\nu)(\Sigma(\nu'+\omega)-U)\Sigma(\nu'+\omega)}{p_1p_2U^2 + (\Sigma(\nu)-p_1U)(\Sigma(\nu'+\omega)-p_1U)} \tag{84}$$

This expression can be shown to be equivalent to the one given in [3].
In the case $\omega = 0$, F becomes a full matrix, which makes solving the Bethe-Salpeter equation for Γ_{ph} harder. It remains possible, even analytically, due to F factorizing.

$$F^{\nu\nu'0} = \beta(1-\delta_{\nu,\nu'})\frac{(\Sigma(\nu)-U)\Sigma(\nu)(\Sigma(\nu')-U)\Sigma(\nu')}{p_1p_2U^2} = (1-\delta_{\nu,\nu'})a(\nu)a(\nu') \tag{85}$$

Where $a(\nu)$ is given by:

$$a(\nu) = \sqrt{\beta}\frac{(\Sigma(\nu)-U)\Sigma(\nu)}{\sqrt{p_1p_2}U}. \tag{86}$$

Inserting this special form into (82) gives us

$$(1-\delta_{\nu,\nu'})a(\nu)a(\nu') = \Gamma_{ph}^{\nu\nu'0} - \frac{1}{\beta}\sum_{\nu_1}\Gamma_{ph}^{\nu\nu_10}G(\nu_1)G(\nu_1)(1-\delta_{\nu_1,\nu'})a(\nu_1)a(\nu'). \tag{87}$$

The summation can be performed for the term $\sim \delta_{\nu_1,\nu'}$, yielding

$$(1-\delta_{\nu,\nu'})a(\nu)a(\nu') = \Gamma_{ph}^{\nu\nu'0} + \frac{1}{\beta}\Gamma_{ph}^{\nu\nu'0}G(\nu')G(\nu')a(\nu')a(\nu') - \frac{1}{\beta}\sum_{\nu_1}\Gamma_{ph}^{\nu\nu_1 0}G(\nu_1)G(\nu_1)a(\nu_1)a(\nu'). \tag{88}$$

Which, in the case $\nu \neq \nu'$ and after a division by $a(\nu')$ can be rewritten as:

$$(a(\nu) + \frac{1}{\beta}\sum_{\nu_1}\Gamma_{ph}^{\nu\nu_1 0}G(\nu_1)G(\nu_1)a(\nu_1)) = \Gamma_{ph}^{\nu\nu'0}(\frac{1}{a(\nu')} + \frac{1}{\beta}G(\nu')G(\nu')a(\nu')) \tag{89}$$

As the left hand side of the equation does not depend on ν', neither can the right hand side. The consequence is, that $\Gamma_{ph}^{\nu\nu'0}$ must factorize when $\nu \neq \nu'$ and moreover, if represented as

$$\Gamma_{ph}^{\nu\nu'0} = b(\nu)b(\nu') - u(\nu)\delta_{\nu,\nu'} \tag{90}$$

where the term $u(\nu)\delta_{\nu,\nu'}$ is intended to absorb the case $\nu = \nu'$, that

$$b(\nu') = \frac{Ca(\nu')}{1 + \frac{1}{\beta}G(\nu')G(\nu')a(\nu')a(\nu'))}. \tag{91}$$

The constant C is left to be determined by entering the expression back into the Bethe-Salpeter equation. Inserting Γ_{ph} back into (82) and evaluating for $\nu \neq \nu'$ and $\nu = \nu'$ yields:

$$a(\nu)a(\nu') = b(\nu)b(\nu') - \frac{1}{\beta}\sum_{\nu_1}(b(\nu)b(\nu_1) - u(\nu)\delta_{\nu,\nu_1})G(\nu_1)G(\nu_1)(1-\delta_{\nu_1,\nu'})a(\nu_1)a(\nu'), \tag{92}$$

$$0 = b(\nu)b(\nu) - u(\nu) - \frac{1}{\beta}\sum_{\nu_1}(b(\nu)b(\nu_1) - u(\nu)\delta_{\nu,\nu_1})G(\nu_1)G(\nu_1)(1-\delta_{\nu_1,\nu})a(\nu_1)a(\nu). \tag{93}$$

From these equations, it is possible to derive

$$u(\nu) = \frac{a^2(\nu)}{1 + \frac{1}{\beta}a^2(\nu)G^2(\nu)}. \tag{94}$$

by setting $\nu = \nu'$ in 93 and taking the difference of the two equations. Upon introducing the constant K

$$K = \frac{1}{\beta}\sum_{\nu_1} b(\nu_1)G(\nu_1)G(\nu_1)a(\nu_1) \tag{95}$$

and inserting the expression 91 into 93, one finds

$$C^2 - CK = 1 \tag{96}$$

and, expressing K via eq. (91) as

$$K = \frac{1}{\beta}\sum_{\nu_1}\frac{Ca(\nu_1)}{1 + \frac{1}{\beta}G(\nu_1)G(\nu_1)a(\nu_1)a(\nu_1))}G(\nu_1)G(\nu_1)a(\nu_1), \tag{97}$$

C can be written as

$$C = \sqrt{\frac{1}{1 - \sum_{\nu_1}\frac{\frac{1}{\beta}G(\nu_1)G(\nu_1)a(\nu_1)a(\nu_1)}{1 + \frac{1}{\beta}G(\nu_1)G(\nu_1)a(\nu_1)a(\nu_1)}}}. \tag{98}$$

The choice of sign for C does not matter, as the quantity appears only squared. As a and G are already known, Γ_{ph} can now be written as:

$$\Gamma_{ph}^{\nu\nu'\omega} = \beta(\delta_{\omega,0}-1)\delta_{\nu,\nu'}\frac{(\Sigma(\nu)-U)\Sigma(\nu)(\Sigma(\nu'+\omega)-U)\Sigma(\nu'+\omega)}{p_1p_2U^2+(\Sigma(\nu)-p_1U)(\Sigma(\nu'+\omega)-p_1U)} + \beta\delta_{\omega,0}$$
$$\left[p_1p_2U^2C^2\frac{(\Sigma(\nu)-U)\Sigma(\nu)}{p_1p_2U^2+(\Sigma(\nu)-p_1U)^2}\frac{(\Sigma(\nu')-U)\Sigma(\nu')}{p_1p_2U^2+(\Sigma(\nu')-p_1U)^2} - \frac{\delta_{\nu,\nu'}(\Sigma(\nu)-U)^2\Sigma^2(\nu)}{p_1p_2U^2+(\Sigma(\nu)-p_1U)^2}\right]. \tag{99}$$

If the contributions from $\omega = 0$ and $\omega \neq 0$ are kept separate. They can, however be added to give:

$$\Gamma_{ph}^{\nu\nu'\omega} = -\beta\delta_{\nu,\nu'}\frac{(\Sigma(\nu)-U)\Sigma(\nu)(\Sigma(\nu'+\omega)-U)\Sigma(\nu'+\omega)}{p_1p_2U^2+(\Sigma(\nu)-p_1U)(\Sigma(\nu'+\omega)-p_1U)} +$$
$$\beta\delta_{\omega,0}p_1p_2U^2C^2\frac{(\Sigma(\nu)-U)\Sigma(\nu)}{p_1p_2U^2+(\Sigma(\nu)-p_1U)^2}\frac{(\Sigma(\nu')-U)\Sigma(\nu')}{p_1p_2U^2+(\Sigma(\nu')-p_1U)^2} \tag{100}$$

As $\Gamma_{ph}^{\nu\nu'\omega}$ can be related to $\Gamma_{\overline{ph}}^{\nu\nu'\omega}$ via the crossing relation, all the irreducible vertices for the Falicov-Kimball model in infinite dimensions are known at this point and the fully irreducible Vertex, Λ, can be expressed.

$$\Lambda^{\nu\nu'\omega} = F^{\nu\nu'\omega} - \sum_c \Phi_c^{\nu\nu'\omega} \tag{101}$$

where the summation is performed over all channels c, and Φ_c denotes the reducible vertex in the respective channel. Since the reducible and irreducible vertex in a given Channel are related via

$$\Gamma_c^{\nu\nu'\omega} + \Phi_c^{\nu\nu'\omega} = F^{\nu\nu'\omega}, \tag{102}$$

it is possible to express Λ in terms of the irreducible vertices and the full vertex:

$$\Lambda^{\nu\nu'\omega} = \sum_c \Gamma_c^{\nu\nu'\omega} - 2F^{\nu\nu'\omega}. \tag{103}$$

If the explicit expressions are inserted, one gets

$$\Lambda^{\nu\nu'\omega} = (\delta_{\omega,0}-\delta_{\nu,\nu'})\beta(\Sigma(\nu)-U)\Sigma(\nu)(\Sigma(\nu'+\omega)-U)\Sigma(\nu'+\omega)\cdot$$
$$\Big[C^2\frac{p_1p_2U^2}{(p_1p_2U^2+(\Sigma(\nu)-p_1U)^2)(p_1p_2U^2+(\Sigma(\nu'+\omega)-p_1U)^2)} +$$
$$2\frac{(\Sigma(\nu)-p_1U)(\Sigma(\nu'+\omega)-p_1U)}{p_1p_2U^2(p_1p_2U^2+(\Sigma(\nu)-p_1U)(\Sigma(\nu'+\omega)-p_1U))}\Big]. \tag{104}$$

Usually, for applying $D\Gamma A$, one would assume this local Λ to be a good approximation for the fully irreducible Vertex of the non-local model and construct the full (non-local) vertex from this and non-local DMFT Green's functions by means of Parquet and Bethe-Salpeter equations. For a fully interacting system, the self-energy could be written in terms of the full vertex by means of the Schwinger-Dyson equation of motion. In the Falicov-Kimball model, this is not possible, as the equation of motion for the self-energy does not contain the interaction vertex for the mobile electrons c but rather the interaction vertex of mobile and localized electrons. For this reason, other ways of generating a non-local self energy out of the known vertex have to be explored.

4.5 Projecting bath states out of the Hamilton operator

The impurity Hamilton operator contains not only site-local terms, but also bath states and couplings with them. It is possible to get rid of the bath states, albeit at the cost of introducing interactions which are non-local in time. To do so, time-dependent creation and annihilation operators have to be Fourier transformed, finding algebraic relations between the transformed operators, allowing for elimination of some of them. The transformation is defined as

$$o\left(\nu\right) = \frac{1}{\beta}\int_0^\beta d\tau e^{i\nu\tau} o\left(\tau\right), \tag{105a}$$

$$o^\dagger(\nu) = \frac{1}{\beta}\int_0^\beta d\tau e^{-i\nu\tau} o^\dagger(\tau). \tag{105b}$$

Here, $o^{(\dagger)}(\tau)$ can be any annihilation (or creation) operator and ν are the fermionic Matsubara frequencies. The inverse transformation is given by

$$o\left(\tau\right) = \sum_\nu e^{-i\nu\tau} o\left(\nu\right), \tag{106a}$$

$$o^\dagger(\tau) = \sum_\nu e^{i\nu\tau} o^\dagger(\nu). \tag{106b}$$

The equations of motion for the bath-state creation and annihilation operators are given by:

$$\frac{d}{d\tau} c_l\left(\tau\right) = \left[\mathcal{H}_{RLM}\,,\, c_l\left(\tau\right)\right], \tag{107a}$$

$$\frac{d}{d\tau} c_l^\dagger(\tau) = \left[\mathcal{H}_{RLM}\,,\, c_l^\dagger(\tau)\right]. \tag{107b}$$

which, when explicitly evaluated, yield:

$$\frac{d}{d\tau} c_l\left(\tau\right) = (\mu - \epsilon_l) c_l\left(\tau\right) + t_l c_i\left(\tau\right), \tag{108a}$$

$$\frac{d}{d\tau} c_l^\dagger(\tau) = (\epsilon_l - \mu) c_l^\dagger(\tau) - t_l^* c_i^\dagger(\tau). \tag{108b}$$

After a Fourier transformation, it is possible to express $c_l\left(\nu\right)$ and $c_l^\dagger(\nu)$ respectively with $c_i\left(\nu\right)$ and $c_i^\dagger(\nu)$

$$c_l\left(\nu\right) = \frac{-t_l c_i\left(\nu\right)}{i\nu - \epsilon_l + \mu}, \tag{109a}$$

$$c_l^\dagger(\nu) = \frac{-t_l^* c_i^\dagger(\nu)}{i\nu - \epsilon_l + \mu}. \tag{109b}$$

The Hamilton operator contains $c_l^{(\dagger)}(\tau = 0)$, which can now be replaced by:

$$c_l\left(\tau = 0\right) = \sum_\nu \frac{-t_l c_i\left(\nu\right)}{i\nu - \epsilon_l + \mu}, \tag{110a}$$

$$c_l^\dagger(\tau = 0) = \sum_\nu \frac{-t_l^* c_i^\dagger(\nu)}{i\nu - \epsilon_l + \mu}. \tag{110b}$$

As the frequency-dependent $c_i^{(\dagger)}(\nu)$ can be written as imaginary time integrals of $c(\tau)$ according to (105b), the hybridization becomes a term which is local in space, at the cost of being non-local in (imaginary) time. The possibility of rewriting the bath operators in terms of the site

operators is not surprising, as knowledge of an actual solution for $c^{(\dagger)}(\tau)$ would be sufficient to render all remaining equations describing the system trivial. The Hamilton operator becomes

$$\mathcal{H}_{RLM} = \varepsilon_f f_i^\dagger f_i + U f_i^\dagger f_i c_i^\dagger c_i - \mu(f_i^\dagger f_i + c_i^\dagger c_i) + \sum_l (\epsilon_l c_l^\dagger c_l) + \sum_l \sum_\nu \frac{t_l^* t_l}{i\nu - \epsilon_l + \mu} \frac{1}{\beta} \int_0^\beta d\tau' \left(c_i^\dagger c_i(\tau') e^{-i\nu\tau'} + c_i^\dagger(\tau') c_i e^{i\nu\tau'} \right). \quad (111)$$

Where the "bath-diagonal" part of the Hamilton operator was deliberately not replaced by an integral expression. One can easily see that above expression contains the definition of the hybridization function, $\Delta(\nu)$, see eq. (62).

$$\mathcal{H}_{RLM} = \varepsilon_f f_i^\dagger f_i + U f_i^\dagger f_i c_i^\dagger c_i - \mu(f_i^\dagger f_i + c_i^\dagger c_i) + \sum_l (\epsilon_l c_l^\dagger c_l) + \sum_\nu \Delta(\nu) \frac{1}{\beta} \int_0^\beta d\tau' \left(c_i^\dagger c_i(\tau') e^{-i\nu\tau'} + c_i^\dagger(\tau') c_i e^{i\nu\tau'} \right). \quad (112)$$

While this form of the Hamilton operator is not very useful for actual calculations as formal problems can arise because the terms $c^{(\dagger_i)}(\tau')$ again depend on the full Hamiltonian. Anyway, the Hamiltonian allows for a interpretation of what a time non-local interaction might mean. Before the substitutions were performed, electrons could move, in the sense that their amplitudes were transported, between the bath- and on-site-states. This possibility is replaced by a transport of amplitudes through time, skipping the explicit amplitudes for being in bath-states. A very similar concept, yet without the issue of definition for $c^{(\dagger_i)}(\tau')$, will be applied to arrive at a time non-local path integral representation for the same problem in section 6.

4.6 Numerical dynamical mean field theory results

In the following section, DMFT results for the Falicov-Kimball model are presented. A DMFT code was written and applied to a Falicov-Kimball model on a three-dimensional lattice with nearest neighbour hopping only. The hopping parameter, t was set to the value $1/(2\sqrt{6})$. Since the impurity model associated with the Falicov-Kimball model can be easily solved analytically as demonstrated in section 4.3, the usual bottleneck of DMFT calculations, i.e. the local impurity solver, does not cause problems here. For high enough temperatures, or equivalently, low enough values of β, the calculations yielded stable and reliable results. Instabilities would appear in the form of the f-electrons vanishing and the c-occupation increasing or vice-versa. This process turned out to be highly sensitive to small changes in the on-site energy for the f-electrons, E_f and the starting conditions. In the paramagnetic phase, both occupations are expected to be at $1/2$ if the chemical potential, μ, and the on-site energy of the f-electrons, E_f are set to

$$\mu = \frac{U}{2} \quad (113a)$$

$$E_f = 0. \quad (113b)$$

This is a consequence of the particle-hole symmetry in such a half filled system. Since the Falicov-Kimball model is known to exhibit phase transitions to charge-ordered phases in 1 and 2 dimensions, the same behaviour is expected in 3 dimensions. DMFT surely is not suitable to describe non-local correlations or properly treat the predicted checkerboard ordering [4], where symmetry breaking occurs. Below, The difference between local c- and f-electron occupation is shown, depending on β and U. A grid of $60 \cdot 60$ points for β and U values was covered, including the first 3000 (positive) Matsubara frequencies and $31^3 k$-points for the evaluation

of the local Green's function. Since fulfilment of equation (113) leads to conservation of the occupations by both c- and f-electrons at a value of 1/2, the reaction of the system to small perturbations was investigated. To this end, separate calculations were initialized with initial values of $p_1 = 0.5 \pm 0.025$, $E_f = 0$ and $\mu = U/2$. After convergence of the c-electron behaviour was achieved, p_1 was updated via

$$p_{1\ new} = \frac{1}{1 + e^{\epsilon_f + U c_{occ} - \mu}} \tag{114}$$

with c_{occ} being the mean c-electron occupation calculated from the c-electron Green's functions. This caused a chain reaction at high enough values of U and at low temperatures, where the f electrons either displaced most of the c-electrons, or were displaced by c electrons themselves. At other sets of parameters, the system converged towards half-filling.

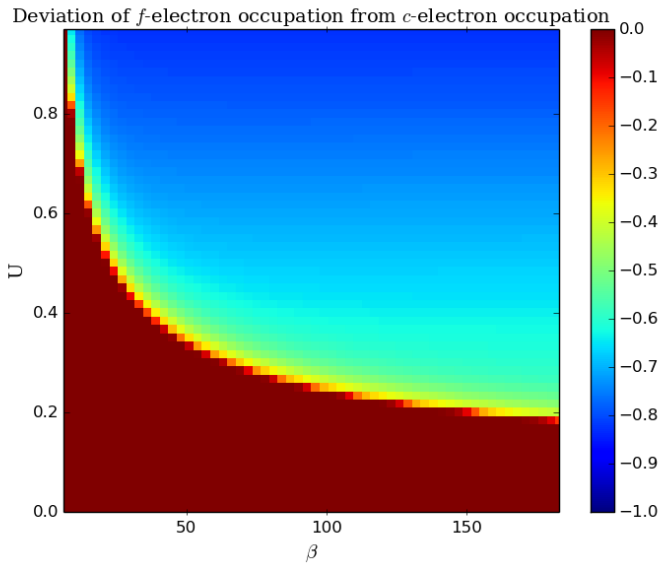

Figure 6: Results of the DMFT calculation for local occupations $n_f - n_c$ starting the iteration from $p_1 = 0.475$ as a function of the interaction U and the inverse temperature β

In Figure 6, one can see where the DMFT calculations show reliable results. When the local occupations by c- and f-electrons are of a similar value, the system is in the paramagnetic, unordered phase. Then, no charge-ordering occurs and DMFT gives reasonable results for the behaviour of the system. When comparing the effects of slightly increased or decreased p_1 as starting condition, one can see a symmetry in the behaviour, depicted in figure 7 . Note that, while the the occupation of f-electrons changes relatively fast from 1/2 to either 0 or 1, the mean occupation by c-electrons is more stable due to the extended density of states. At low temperatures, these grand-canonical calculations at fixed μ showed a tendency towards "ferro" ordering with predominantly c- or f-electrons. Those solutions of the DMFT cycle do not conserve the total occupancy $n_f + n_c$ of the system, which makes them less stable, they are a consequence the single-site treatment of the problem DMFT offers which facilitates such ordering.

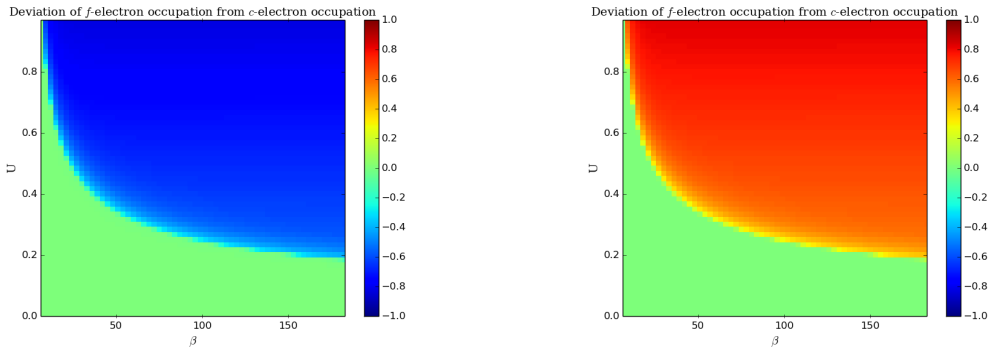

Figure 7: Same as figure 6, but for a starting value of p_1 slightly smaller and greater than 1/2

Another set at calculations was performed, this time at fixed half filling,

$$n_f = n_c = \frac{1}{2}, \tag{115}$$

for the particle-hole symmetric case $\mu = U/2$, $E_f = 0$. The converged results where used as raw data for the self-energy when investigating the vertices calculated in section 4.4.

5 Structure of the vertices in local approximation and derived quantities

Using the local vertices from section 4, one can devise different approximations for describing the vertices of the actual Falicov-Kimball model. The aim of this chapter is to investigate the structure of the vertices resulting from the DMFT approach as well as the results of different approximations for the full problem. The behaviour of the vertices is relevant especially when considering the effects of approximations necessitated by the use of computers, for example finite Matsubara-frequency ranges and their influence on the total result. The discussions of the vertices will be accompanied by heat-plots of the real parts of the vertices in question for the energy transfer $\omega = 0$, resulting from a DMFT calculation at $\beta = 25$ and $U = 0.2$ at fixed f-electron filling $p_1 = 1/2$, as well as a second set at $\beta = 72$, illustrating the main features of the vertices and how they change when approaching the phase transition towards a checkerboard-ordered phase. Our energy scale is set by $t = 1/(2\sqrt{6})$. When p_1 is fixed to a value of $1/2$ and μ is set to $\mu = U/2$, the vertices are purely real.

5.1 Asymptotic behaviour of the local vertices from the DMFT calculation

5.1.1 Full vertex F

First, the full local vertex F is investigated. The analytic expression for the vertex, according to section 4 is given by:

$$F^{\nu\nu'\omega} = \beta(\delta_{\omega,0} - \delta_{\nu,\nu'})\frac{(\Sigma(\nu) - U)\Sigma(\nu)(\Sigma(\nu' + \omega) - U)\Sigma(\nu' + \omega)}{p_1 p_2 U^2}. \tag{116}$$

Obviously, the vertex is only non-zero when either $\omega = 0$ or $\nu = \nu'$. Thus, only the limits of $\omega \to \pm\infty$ when $\nu = \nu'$, or either $\nu \to \pm\infty$, $\nu' \to \pm\infty$ or both, when $\omega = 0$ are regarded in the following. As this behaviour is common to all of the calculated vertices, i.e. the reducible as well as irreducible ones, the same procedure will be followed for all of them.
When ω is set to zero, one needs to investigate the asymptotic behaviour of

$$(\Sigma(\nu) - U)\,\Sigma(\nu). \tag{117}$$

As $\nu \to \pm\infty$, $\Sigma(\nu)$ approaches $p_1 U$ as can be seen from equation (67). The asymptotic form of the full Vertex then becomes:

$$F^{\pm\infty\,\nu'0} = -\beta(\Sigma(\nu') - U)\Sigma(\nu') \tag{118}$$

When $\nu' \to \pm\infty$ as well, F converges to a constant value of

$$F^{\pm\infty\pm\infty\,0} = \beta p_1 p_2 U^2, \tag{119}$$

which means that a truncation of a summation over F will not yield meaningful results unless other terms cause convergence.
When ν is set equal to ν', the asymptotic behaviour in ω is described by:

$$F^{\nu\nu\pm\infty} = \beta(\Sigma(\nu) - U)\Sigma(\nu) \tag{120}$$

When investigating the limit $\nu \to \pm\infty$ as well, F approaches

$$F^{\pm\infty\pm\infty\pm\infty} = -\beta p_1 p_2 U^2 \tag{121}$$

It is worth mentioning that the asymptotic behaviour of the full vertex deviates from what one might expect when considering the vertices of the Hubbard model. The constant term that the

vertex converges to is $\beta p_1 p_2 U^2$ instead of just U. This is a consequence of the c-electrons, which are described by this vertex, not interacting directly; two "messenger" f-electron propagators are needed to connect c-electron lines to each other.

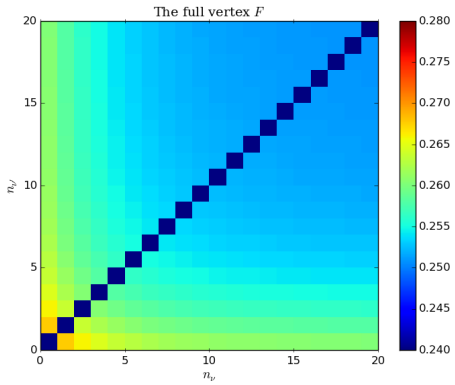

Figure 8: Full vertex when $\omega = 0$ and $\beta = 25$, n_ν and $n_{\nu'}$ give the number of the Matsubara frequencies, according to eq. (23)

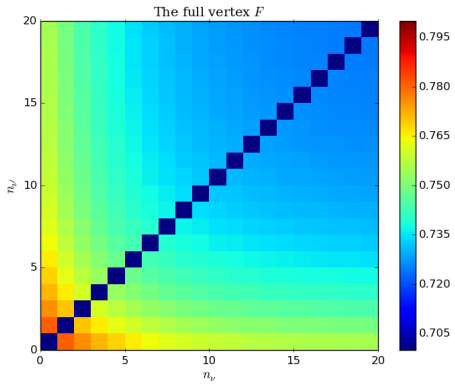

Figure 9: Full vertex when $\omega = 0$ and $\beta = 72$, n_ν and $n_{\nu'}$ give the number of the Matsubara frequencies, according to eq. (23)

In figure 8 and 9 one can see the features of F. It is identically equal to zero along the main diagonals and converges towards a value of 0.25 or 0.72 for large ν and ν', as predicted by the value of $\beta p_1 p_2 U^2$. Note that the scales are different for the figures and a lower cut-off was introduced on the colour scale, allowing for a better recognizability of the values which are not 0.

5.1.2 Particle-particle irreducible vertex Γ_{pp}

The particle-particle irreducible vertex is given by:

$$\Gamma_{pp}^{\nu\nu'\omega} = \beta(\delta_{\omega,0} - \delta_{\nu,\nu'})\frac{(\Sigma(\nu) - U)\Sigma(\nu)(\Sigma(\nu'+\omega) - U)\Sigma(\nu'+\omega)}{p_1 p_2 U^2 + (\Sigma(\nu) - p_1 U)(\Sigma(\nu'+\omega) - p_1 U)} \tag{122}$$

Setting ω to zero, the vertex is

$$\Gamma_{pp}^{\nu\nu' 0} = \beta\frac{(\Sigma(\nu) - U)\Sigma(\nu)(\Sigma(\nu') - U)\Sigma(\nu')}{p_1 p_2 U^2 + (\Sigma(\nu) - p_1 U)(\Sigma(\nu') - p_1 U)}, \tag{123}$$

yielding, for $\nu \to \pm\infty$

$$\Gamma_{pp}^{\pm\infty\,\nu' 0} = -\beta(\Sigma(\nu') - U)\Sigma(\nu'). \tag{124}$$

In the limes of $\nu' \to \pm\infty$ this expression approaches the value for the asymptotic full vertex:

$$\Gamma_{pp}^{\pm\infty\pm\infty\,0} = \beta p_1 p_2 U^2 \tag{125}$$

When regarding the term proportional to $\delta_{\nu,\nu'}$ for $\omega \to \pm\infty$, the expression

$$\Gamma_{pp}^{\nu\nu\pm\infty} = \beta(\Sigma(\nu) - U)\Sigma(\nu) \tag{126}$$

is recovered. When taking the limit of $\nu \to \pm\infty$ as well, one gets:

$$\Gamma_{pp}^{\pm\infty\pm\infty\pm\infty} = -p_1 p_2 U^2 \tag{127}$$

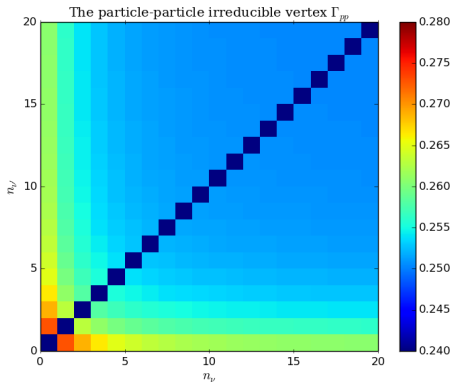

Figure 10: same as 8 but for the particle-particle irreducible vertex

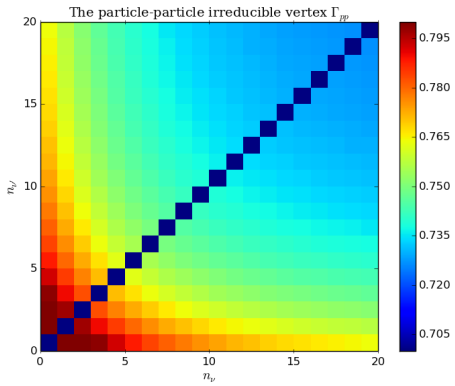

Figure 11: same as 9 but for the particle-particle irreducible vertex

Figures 10 and 11 display the features of the particle-particle irreducible vertices. They are very similar to the according full vertices and thus have been plotted utilizing the same scaling.

5.1.3 Particle-hole irreducible vertex Γ_{ph}

The local particle-hole irreducible vertex Γ_{ph} is given by

$$\Gamma_{ph}^{\nu\nu'\omega} = -\beta\delta_{\nu,\nu'}\frac{(\Sigma(\nu)-U)\Sigma(\nu)(\Sigma(\nu'+\omega)-U)\Sigma(\nu'+\omega)}{p_1p_2U^2+(\Sigma(\nu)-p_1U)(\Sigma(\nu'+\omega)-p_1U)}+ \\ \beta\delta_{\omega,0}p_1p_2U^2C^2\frac{(\Sigma(\nu)-U)\Sigma(\nu)}{p_1p_2U^2+(\Sigma(\nu)-p_1U)^2}\frac{(\Sigma(\nu')-U)\Sigma(\nu')}{p_1p_2U^2+(\Sigma(\nu')-p_1U)^2} \tag{128}$$

While the contribution proportional to $\delta_{\nu,\nu'}$ approaches

$$\Gamma_{ph}^{\nu\nu\pm\infty} = \beta(\Sigma(\nu)-U)\Sigma(\nu) \tag{129}$$

as ω goes to infinity, the one stemming from $\delta_{\omega,0}$ leads to the following expression in the limes $\nu \to \pm\infty$:

$$\Gamma_{ph}^{\pm\infty\,\nu'0} = -\beta\delta_{\omega,0}p_1p_2U^2C^2\frac{(\Sigma(\nu')-U)\Sigma(\nu')}{p_1p_2U^2+(\Sigma(\nu')-p_1U)^2}. \tag{130}$$

If $\nu' \to \pm\infty$ as well, Γ_{ph} becomes

$$\Gamma_{ph}^{\pm\infty\pm\infty\,0} = \beta C^2 p_1p_2U^2. \tag{131}$$

Because $\Gamma_{\overline{ph}}$ and Γ_{ph} are related via equation (81), the limit of $\Gamma_{\overline{ph}}$ need not be treated explicitly.

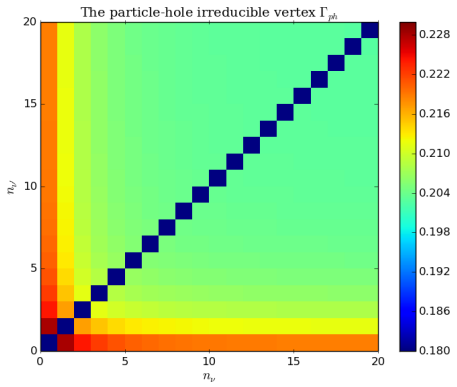

Figure 12: same as 8 but for the particle-hole irreducible vertex

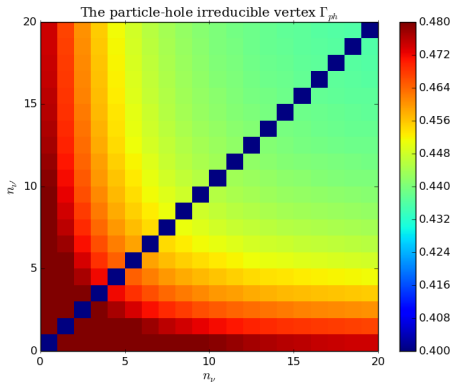

Figure 13: same as 9 but for the particle-particle irreducible vertex

Figures 12 and 13 illustrate the behaviour of the particle-hole irreducible vertex. It converges towards a different value than the full vertex and the *pp*-irreducible one.
Also, the factor C^2 appearing in the direct part (proportional to $\delta_{\omega,0}$) of the *ph*-irreducible vertex and by extension, the $\overline{ph}$-irreducible and fully irreducible vertex, has been plotted on the same grid as figure 7 in figure 14

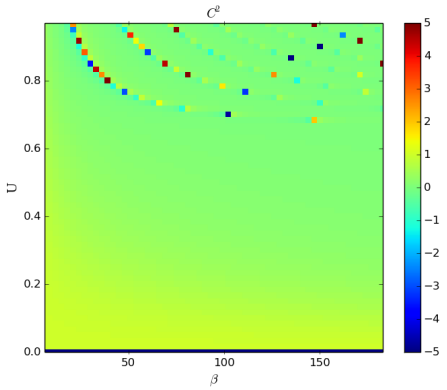

Figure 14: Results of the DMFT calculation for C^2

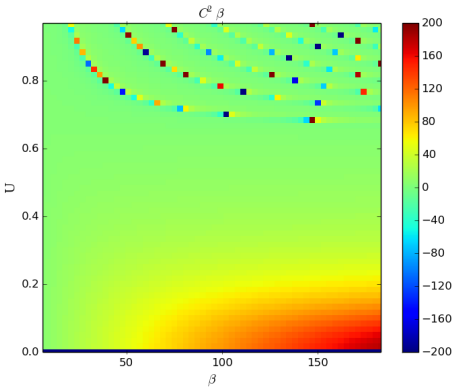

Figure 15: Results of the DMFT calculation for $C^2 \cdot \beta$

It is to be noted, that when *plotting* C^2 in Figure 14, a cut-off was introduced, setting values larger than 5 to 5, thus allowing for better recognisability. As C^2 appears only with a pre-factor of β, this quantity was plotted as well. As Figure 15 shows, $C^2 \cdot \beta$ diverges for high values of U. Thus, the local fully irreducible vertex is also enhanced in these regions. A similar phenomenon has been observed in the literature for the Hubbard [13] and the Falicov-Kimball [14] models.

5.1.4 Fully irreducible vertex Λ

As established in section 4, Λ can be written as:

$$\Lambda^{\nu\nu'\omega} = (\delta_{\omega,0} - \delta_{\nu,\nu'})\beta(\Sigma(\nu) - U)\Sigma(\nu)(\Sigma(\nu' + \omega) - U)\Sigma(\nu' + \omega)$$
$$\Big[C^2 \frac{p_1 p_2 U^2}{(p_1 p_2 U^2 + (\Sigma(\nu) - p_1 U)^2)(p_1 p_2 U^2 + (\Sigma(\nu' + \omega) - p_1 U)^2)} +$$
$$2\frac{(\Sigma(\nu) - p_1 U)(\Sigma(\nu' + \omega) - p_1 U)}{p_1 p_2 U^2 (p_1 p_2 U^2 + (\Sigma(\nu) - p_1 U)(\Sigma(\nu' + \omega) - p_1 U))}\Big]. \quad (132)$$

When ω is again set to zero, the asymptotic behaviour for large ν is given by:

$$\Lambda^{\pm\infty\,\nu'0} = -\beta p_1 p_2 U^2 (\Sigma(\nu') - U)\Sigma(\nu')\; C^2 \frac{1}{(p_1 p_2 U^2 + (\Sigma(\nu') - p_1 U)^2)} \tag{133}$$

When $\nu' \to \pm\infty$ as well, Λ yields the already familiar expression:

$$\Lambda^{\pm\infty\pm\infty\,0} = \beta p_1 C^2 p_2 U^2 \tag{134}$$

A treatment of large values of ω when $\nu = \nu'$ results in

$$\Lambda^{\nu\nu\pm\infty} = \beta p_1 p_2 U^2 (\Sigma(\nu) - U)\Sigma(\nu)\; C^2 \frac{1}{(p_1 p_2 U^2 - (\Sigma(\nu) - p_1 U)^2)} \tag{135}$$

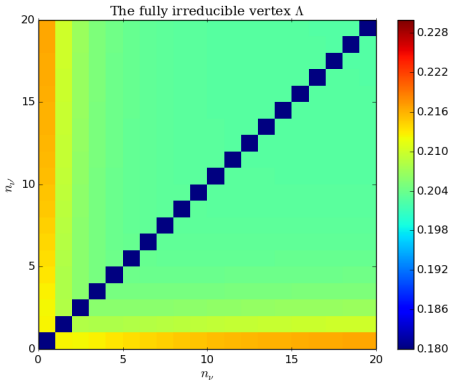

Figure 16: same as 8 but for the fully irreducible vertex

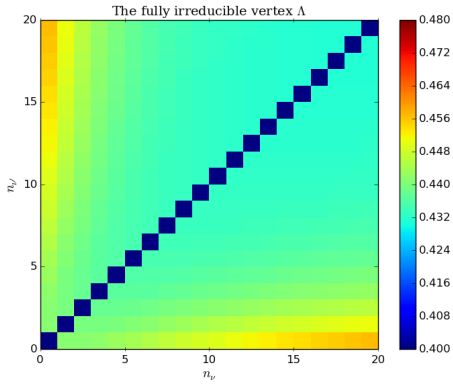

Figure 17: same as 9 but for the fully irreducible vertex

The main features of the local fully irreducible vertex can be seen in figures 16 and 17. The fully irreducible vertex, in contrast to the full vertex and the channel-irreducible ones, displays larger deviations from the value it approaches in its limits where one of the fermionic Matsubara frequencies is small, but the other one is not. The scales have been chosen consistently with the ones for the corresponding *ph*-irreducible vertices.

5.2 Ladder approximations for the full momentum dependent vertex F

If the vertex irreducible in a given channel c, Γ_c, is assumed to be local, the corresponding Bethe-Salpeter equation can be used to construct a momentum dependent vertex out of Γ_c and non-local DMFT Green's functions. For convenience, the calculations are performed in momentum, instead of real space. Approximating Γ_c by its local counterpart means that Γ_c scatters two incident particles equally into all pairs of states which obey conservation of momentum. This in turn causes the full vertex to be dependent on the momentum transfer only, but not on the explicit momenta of the incoming or outgoing particles, when building a particle-hole or transverse particle-hole ladder, while a particle-particle ladder leads to a dependency on the total momentum of the involved particles. Assuming one knows the explicit form of the momentum dependent Green's functions, $G(\nu, k)$, the Bethe-Salpeter equations can be solved analytically in the approximation of a local Γ_c. Starting with the ladder approximation in the particle-particle channel, this will be done in the following section. As special interest exists for the k-points

$(0,0,0)$, usually called Γ, and (π,π,π), they are defined as:

$$q = 0 = \begin{pmatrix} 0 \\ 0 \\ 0 \end{pmatrix} \tag{136a}$$

$$q = \Pi = \begin{pmatrix} \pi \\ \pi \\ \pi \end{pmatrix} \tag{136b}$$

Where Γ was relabelled as 0 to avoid confusion with the irreducible vertices.

5.2.1 Particle-particle ladder

Assuming the local Γ_{pp} as derived for the resonant level model is a good approximation for the particle-particle irreducible vertex of the full Falicov-Kimball model, the Bethe Salpeter equation in the particle-particle channel, in particle-particle notation takes the form:

$$F^{\nu\nu'\omega}_{q,pp} = \Gamma^{\nu\nu'\omega}_{pp} + \frac{1}{2\beta}\sum_{\nu_1,k_1} F^{\nu(\omega-\nu_1)\omega}_{q} G(\nu_1,k_1)G(\omega-\nu_1,q-k_1)\Gamma^{(\nu_1)\nu'\omega}_{pp} \tag{137}$$

Where Γ_{pp} is understood to be the particle-particle irreducible vertex and q is the total momentum transfer. In particle-particle notation, Γ_{pp} is known to have a "cross-structure" in ν and ν'. Inserting the known form from equation (79) for Γ_{pp} leads to:

$$F^{\nu\nu'\omega}_{q,pp} = \frac{\Gamma^{\nu\nu'\omega}_{pp}}{1 - \frac{1}{2\beta}\tilde{\Gamma}^{\nu\nu'\omega}_{pp}\sum_{k_1}(G(\omega-\nu',k_1)G(\nu',q-k_1) + G(\nu',k_1)G(\omega-\nu',q-k_1))} \tag{138}$$

Transforming back to particle-hole notation, except for the parameter q, which is left in its pp-notation meaning, the total momentum of the particles involved into the scattering process, gives us

$$F^{\nu\nu'\omega}_{q\,ph} = \frac{\Gamma^{\nu\nu'\omega}_{pp}}{1 - \frac{1}{2\beta}\tilde{\Gamma}^{\nu\nu'\omega}_{pp}\sum_{k_1}(G(\omega+\nu,k_1)G(\nu',q-k_1) + G(\nu',k_1)G(\omega+\nu,q-k))}. \tag{139}$$

The resulting, momentum-dependent full vertex has the same structure regarding the frequencies ν,ν' and ω as the original, local one. Note that the expression

$$\sum_{k_1}(G(\omega+\nu,k_1)G(\nu',q-k_1) + G(\nu',k_1)G(\omega+\nu,q-k_1)) \tag{140}$$

can easily be shown to be equal to

$$2\sum_{k_1} G(\omega+\nu,k_1)G(\nu',q-k_1) \tag{141}$$

by performing an index shift $k_1 \to q - k'$. It turns out to be convenient to define

$$\chi_0(\nu,\nu',\omega,q) = \frac{1}{\beta}\sum_{k_1} G(\nu,k_1)G(\nu'+\omega,k_1+q), \tag{142}$$

allowing for rewriting the expression for the full vertex in the particle-particle approximation as

$$F^{\nu\nu'\omega}_{q\,ph} = \frac{\Gamma^{\nu\nu'\omega}}{1 - \tilde{\Gamma}^{\nu\nu'\omega}\chi_0(\nu,\nu',\omega,q)} \tag{143}$$

if the system shows space-inversion symmetry.

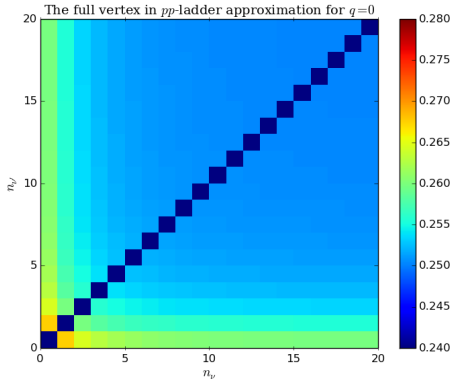

Figure 18: Full vertex in *pp*-ladder approximation when $\omega = 0$, $\beta = 25$ and $q = 0$, n_ν and $n_{\nu'}$ give the number of the Matsubara frequencies, according to eq. (23)

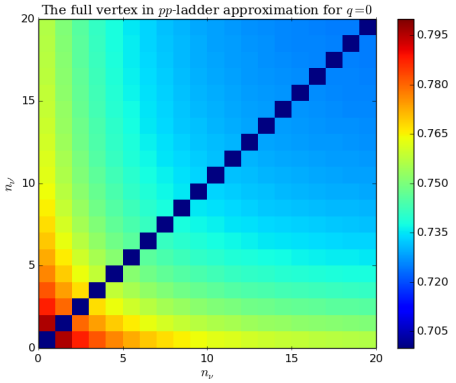

Figure 19: Full vertex in *pp*-ladder approximation when $\omega = 0$, $\beta = 72$ and $q = 0$, n_ν and $n_{\nu'}$ give the number of the Matsubara frequencies, according to eq. (23)

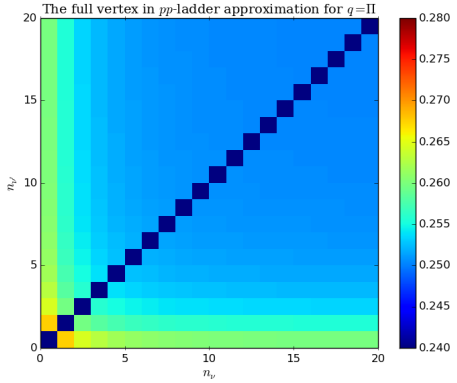

Figure 20: same as 18 but for $q = \Pi$

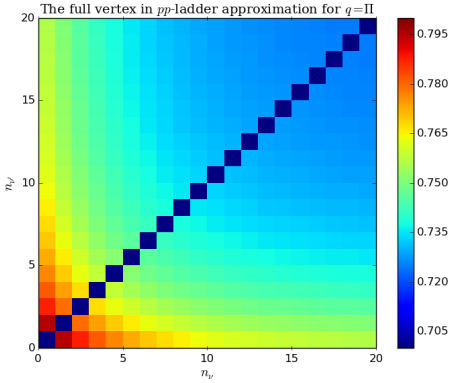

Figure 21: same as 19 but for $q = \Pi$

Figures 18 - 21 display the full vertex one obtains from *pp*-ladder approximation. The vertices look very similar to the original local ones, despite being momentum-dependent objects now. Also, hardly any difference is noticeable between evaluation for the total momentum being 0 or Π. This weak dependence on q is a consequence of the minor role *pp*-effects play for the Falicov-Kimball model in this parameter regime, while a more pronounced dependency would be expected when describing Anderson localization.

5.2.2 Particle-hole ladder

The Bethe-Salpeter equation in the particle-hole channel, using non-local DMFT Green's functions, but keeping Γ_{ph} local (i.e. the DMFT Γ_{ph}) has the following form:

$$F_q^{\nu\nu'\omega} = \Gamma_{ph}^{\nu\nu'\omega} - \frac{1}{\beta}\sum_{\nu_1,k_1} \Gamma_{ph}^{\nu\nu_1\omega} G(\nu_1,k_1)G(\nu_1+\omega,k_1+q)F_q^{\nu_1\nu'\omega} \tag{144}$$

The equation can be solved, using the analytic expression for Γ_{ph} derived in section 4.4. It can be shown that, due to Γ_{ph} being of the form

$$\Gamma_{ph}^{\nu\nu'\omega} = \delta_{\omega,0} b(\nu) b(\nu') - \delta_{\nu,\nu'} u(\nu,\omega), \tag{145}$$

$F_q^{\nu\nu'\omega}$ must have the structure

$$F_q^{\nu\nu'\omega} = \delta_{\omega,0} \widetilde{a}(\nu,q) \widetilde{a}(\nu',q) - \delta_{\nu,\nu'} f(\nu,\omega,q) \tag{146}$$

by similar arguments as those leading to equation (90). Note that the function $\widetilde{a}$ is now different from, albeit similar to, the function a in section 4.4. Inserting this form for F and Γ_{ph}, which is already known, then proceeding with similar calculations to the ones yielding Γ_{ph} in section 4.4, one arrives at:

$$f(\nu,\omega,q) = \frac{u(\nu,\omega)}{1 - u(\nu,\omega)\chi_0(\nu,\nu,\omega,q)}, \tag{147}$$

and

$$\widetilde{a}(\nu,q) = C_q \frac{b(\nu)}{1 - u(\nu,0)\chi_0(\nu,\nu,0,q)}, \tag{148}$$

with the quantity C_q defined as:

$$C_q{}^2 = \frac{1}{1 + \sum_{\nu_1} \frac{b^2(\nu_1)\chi_0(\nu_1,\nu_1,0,q)}{1 - u(\nu_1,0)\chi_0(\nu_1,\nu_1,0,q)}}. \tag{149}$$

This leads to the following expression for the full vertex:

$$F_q^{\nu\nu'\omega} = \delta_{\omega,0} C_q{}^2 \frac{b(\nu)b(\nu')}{(1 - u(\nu,0)\chi_0(\nu,\nu,0,q))(1 - u(\nu',0)\chi_0(\nu',\nu',0,q))} - \delta_{\nu,\nu'} \frac{u(\nu,\omega)}{1 - u(\nu,\omega)\chi_0(\nu,\nu,\omega,q)} \tag{150}$$

Note that this specific approximation leads to a F which breaks the crossing symmetry. Such an F surely cannot always be a good approximation for the actual full vertex of the Falicov-Kimball model, and, hence, one has to be careful about the restrictions on the described physics.

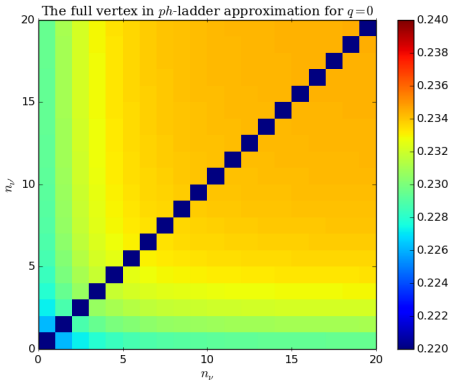

Figure 22: Full vertex in *ph*-ladder approximation when $\omega = 0$, $\beta = 25$ and $q = 0$, n_ν and $n_{\nu'}$ give the number of the Matsubara frequencies, according to eq. (23)

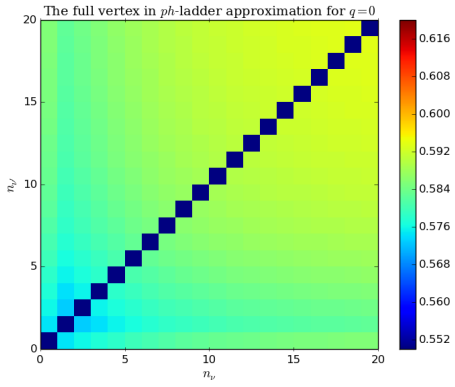

Figure 23: Full vertex in *pp*-ladder approximation when $\omega = 0$, $\beta = 72$ and $q = 0$, n_ν and $n_{\nu'}$ give the number of the Matsubara frequencies, according to eq. (23)

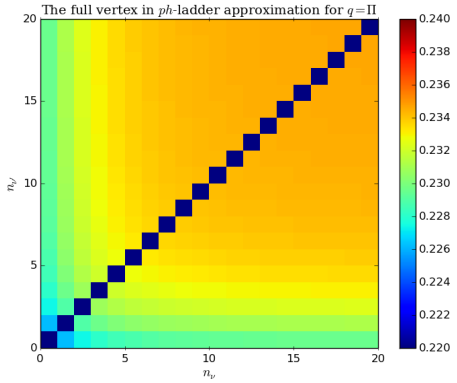

Figure 24: Same as 22 but for $q = \Pi$

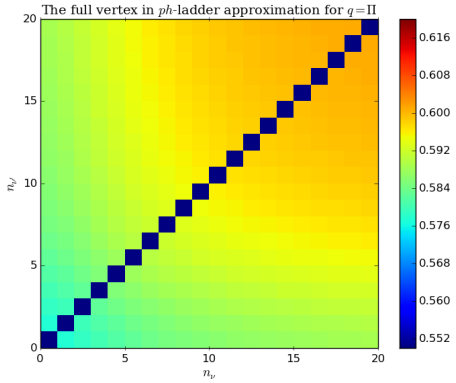

Figure 25: Same as 23 but for $q = \Pi$

The full, momentum-dependent vertices extracted from a particle-hole ladder are given in figures 22 - 25 . Their behaviour differs from the local full vertices, even inverting the trend for which values of n_ν and $n_{\nu'}$ to expect larger values of the vertex. Unlike the pp-ladder, the ph-ladder shows pronounced momentum-dependence in the full vertex near the phase transition.

5.3 Susceptibilities

From the full vertices calculated by the different ladder approximations, it is possible to extract susceptibilities for c-electrons. Since, these susceptibilities are given by

$$\chi^{\nu,\nu',\omega}_{k,k',q} = -\beta G(\nu,k)G(\nu+\omega,k+q)\delta_{\nu,\nu'}\delta_{k,k'} + G(\nu+\omega,k+q)G(\nu',k')F^{\nu\nu'\omega}_q G(\nu'+\omega,k'+q)G(\nu,k), \tag{151}$$

their behaviour will depend mainly on the structure of F. Specifically, divergence of the susceptibilities is to be expected whenever F diverges. Thus, the denominators of the different expressions for F are investigated. Two types of divergences can occur, when either C_q goes to infinity at a certain value of q, or when the expression

$$1 - \chi_0(\nu,\nu',\omega,q)\frac{(\Sigma(\nu)-U)\Sigma(\nu)(\Sigma(\nu'+\omega)-U)\Sigma(\nu'+\omega)}{p_1p_2U^2 + (\Sigma(\nu)-p_1U)(\Sigma(\nu'+\omega)-p_1U)} \tag{152}$$

comes close to 0, since it appears as a denominator in the full vertex extracted from the particle-particle, as well as the particle-hole ladder. To extract physically observable, macroscopic susceptibilities, one has to sum over all values of ν , ν' , k and k', since one is typically only interested in the correlation effects for probabilities of finding electrons at given relative positions in space and time. A Fourier transform in these relative coordinates leads to a momentum and frequency dependence.

$$\chi^{physical}_q(\omega) = \frac{1}{\beta^2 N}\sum_{\nu,\nu',k,k'} \chi^{\nu,\nu',\omega}_{k,k',q} \tag{153}$$

N is the total number of distinct lattice sites, or equivalently, k-points. When investigating phase transitions, ω can be set to 0. For the half-filled system, divergences in the susceptibility are expected to occur at the q-vector

$$q = \Pi = \begin{pmatrix} \pi \\ \pi \\ \pi \end{pmatrix} \tag{154}$$

when the system condenses into checkerboard ordering.

5.4 Numerical results

In this subsection, numerical results obtained from inserting converged quantities resulting from DMFT into the expressions already derived will be discussed. These calculations have been performed at a fixed f-electron filling of $1/2$, thus ensuring the c-occupation is fixed at $1/2$ as well and precluding a DMFT phase separation in the system from occurring. First, the purely DMFT charge susceptibility

$$\chi^{\nu,\nu',\omega}_{k,k',q} = -\beta G(\nu,k)G(\nu+\omega,k+q)\delta_{\nu,\nu'}\delta_{k,k'} + G(\nu+\omega,k+q)G(\nu',k')F^{\nu\nu'\omega}G(\nu'+\omega,k'+q)G(\nu,k), \tag{155}$$

is calculated, using the self-consistent results from the DMFT calculation for Σ to express G and F. While the dispersion relation of the system is used for updating the Green's function within the DMFT-self consistency, the full vertex is replaced by its local counterpart for the calculation of the susceptibility. Such a calculation can be performed very fast, yet the results carry little information. Better results are expected when using a momentum-dependent full vertex, such as the ones extracted from local Γs and Bethe-Salpeter equations above. Divergencies can occur here, as Γ is a part of a geometric series in this context. Generally, the particle-hole ladder approximation is used, as one is interested in charge order instabilities. Since the operator of electron-occupation at the (real) time t and position i is given by $c^\dagger_i(t)c_i(t)$, the physical susceptibility one is interested in, is given by the expectation value of the operator $c^\dagger_i(t)c_i(t)c^\dagger_j(t')c_j(t')$. In terms of propagators, the connected parts of this expectation value consist of correlated transport of an electron and an electron-hole.

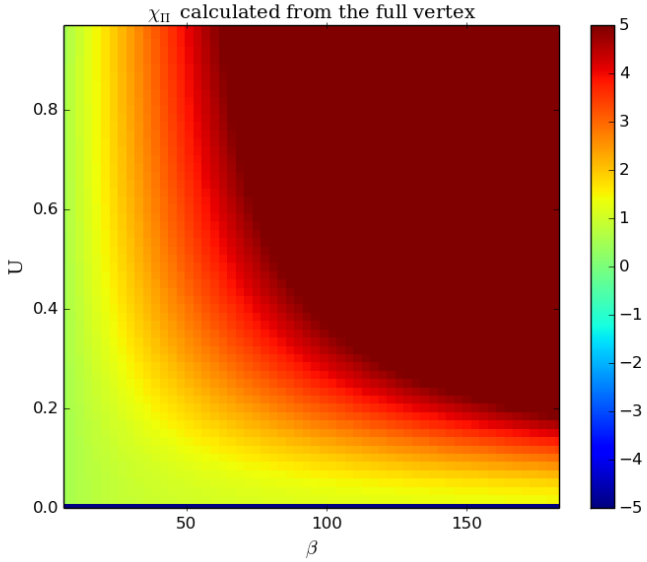

Figure 26: Charge susceptibility at the wave vector (π,π,π) , χ_Π, calculated using the full local vertex F as basis

In figure 26 one can clearly see that no divergencies occur in the susceptibility χ_Π when the purely local (full) vertex is used for the calculation. Note that values above 5 have been set to 5 for the sake of a better readability of the plot. The system does however show a first tendency of ordering, recognizable by the χ_Π becoming larger at high values of U and low temperatures.

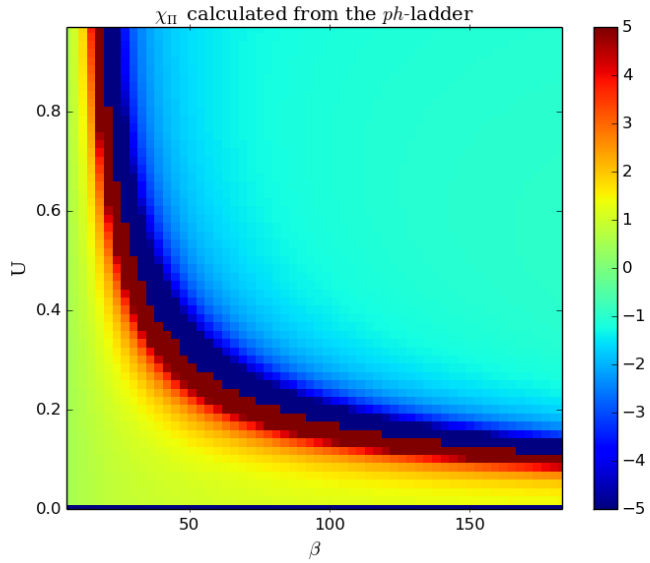

Figure 27: Charge susceptibility at the wave vector (π, π, π), χ_Π, calculated using the full vertex calculated from the ph-ladder F_q as basis

Figure 27 shows divergencies for χ_Π when a ph-ladder approximation is made for the full vertex. After the divergence occurs, the susceptibility shifts to negative, non-physical values. Besides the low-temperature and small U limits described so far, the charge density wave susceptibility was calculated on a T-U grid for an extended region. Points of divergence where calculated and a second order spline was used to interpolate the curve of diverging susceptibility. The resulting phase diagram, figure 28 is the DMFT phase diagram since the leading term for the physical susceptibility in $1/d$ with d being the dimensionality of the system, is the ph-ladder based on the local ph-irreducible vertex. For low temperatures, the value of U where a transition occurs varies linearly with T, in agreement with the $1/\beta$ behaviour observed before. A critical value of U, U_{crit}, exists, where the critical temperature reaches its maximum.

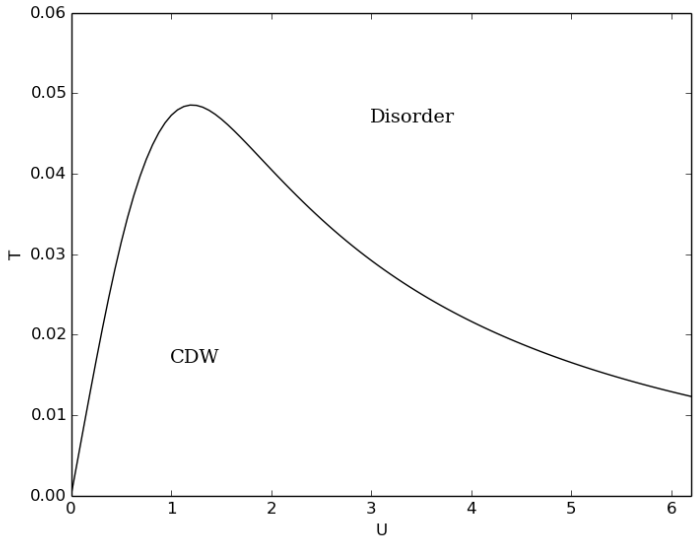

Figure 28: Phase diagram of the Falicov-Kimball model within DMFT using the ph-ladder approximation with the local ph-irreducible vertex

The behaviour of the Falicov-Kimball model is intuitive for low values of U and T, where an increase in U can cause the system to order, while an increase of temperature increases the tendency of disorder. When increasing U beyond the value $U_{crit} \sim 2dt$, the critical temperature becomes lower again. U_{crit} has a value similar to the bandwidth of the non-interacting system. When the Hubbard-bands begin separating, movement of c-electrons between sites occupied and unoccupied by f-electrons is hindered, thus preventing long-ranged order from arising.

6 Path integral approaches

A controlled way of using DMFT results as a starting point for calculation of non-local correlation effects for a finite-dimensional (typically in two or three dimensions) Falicov-Kimball model is possible when adopting a path integral formulation of the Green's functions. To this end, because fermions are to be described, Grassmann numbers and integration have to be introduced. Instead of writing products over integrals for different Matsubara Frequencies, a capital D is used as shorthand notation for the multi-dimensional infinitesimal Volumes element. The grand-canonical partition function Z for the Falicov-Kimball model in Path integral representation reads:

$$Z = \int \prod_i Dc_i^\dagger Dc_i Df_i^\dagger Df_i e^{-S(c^\dagger,c,f^\dagger,f)} \tag{156}$$

with S being the action of the Falicov-Kimball model,

$$S = \int_0^\beta d\tau \left[\sum_i \left(c_i^\dagger \frac{d}{d\tau} c_i + f_i^\dagger \frac{d}{d\tau} f_i + U c_i^\dagger c_i f_i^\dagger f_i \right) - t \sum_{\langle i,j \rangle} c_i^\dagger c_j \right]. \tag{157}$$

The index i again goes over all lattice sites, while $\langle i, j \rangle$ includes all pairs of nearest neighbours. The Grassmann fields $c^{(\dagger)}$ and $f^{(\dagger)}$ are functions of the imaginary time. While this integral cannot be performed analytically, it is possible to rewrite the exponent in terms of the action of the associated resonant level model and additive correction terms. While the solution of the first part is known, a controlled approximation for the second one can be derived. The action of the resonant level model for a single site i can be written as

$$S = \int_0^\beta d\tau \left[(c_i^\dagger \frac{d}{d\tau} c_i + f_i^\dagger \frac{d}{d\tau} f_i + U c_i^\dagger c_i f_i^\dagger f_i + \sum_l (c_l^\dagger \frac{d}{d\tau} c_l + \epsilon_l c_l^\dagger c_l - t_l c_l^\dagger c_i - t_l^* c_i^\dagger c_l) \right]. \tag{158}$$

Where i is the index of the site in question and l are the indices of the bath-states.

6.1 Integrating out bath states from the action of the resonant level model

Just as the resonant level model Hamilton operator allows for elimination of bath-state operators, the action functional allows one to integrate out their Grassmann fields. To this end, it is convenient to transform the time-dependent Grassmann fields associated with creation and annihilation operators to frequency space. The transformation is defined as

$$o(\nu) = \frac{1}{\beta} \int_0^\beta d\tau e^{i\nu\tau} o(\tau), \tag{159a}$$

$$o^\dagger(\nu) = \frac{1}{\beta} \int_0^\beta d\tau e^{-i\nu\tau} o^\dagger(\tau). \tag{159b}$$

Here, $o^{(\dagger)}(\tau)$ can be any Grassmann field and ν are the fermionic Matsubara frequencies. The inverse transformation is given by

$$o(\tau) = \sum_\nu e^{-i\nu\tau} o(\nu), \tag{160a}$$

$$o^\dagger(\tau) = \sum_\nu e^{i\nu\tau} o^\dagger(\nu). \tag{160b}$$

The action, expressed in frequency-dependent Grassmann fields, except for the interaction part between c and f electrons, then becomes

$$S_{RLM} = \sum_\nu \left[-i\nu c_i^\dagger c_i - i\nu f_i^\dagger f_i + \sum_l \left(-i\nu c_l^\dagger c_l + \epsilon_l c_l^\dagger c_l - t_l c_l^\dagger c_i - t_l^* c_i^\dagger c_l \right) \right] + \int_0^\beta d\tau U c_i^\dagger(\tau) c_i(\tau) f_i^\dagger(\tau) f_i(\tau). \tag{161}$$

In equation (161), all fields which are not explicitly denoted as time-dependent are assumed to be frequency-dependent. Since the bath-states now appear in a Gaussian way, they can be integrated out, leading to multiplicative factors in the partition function, which can be neglected when calculating expectation values, and a modification of the remaining part of the action.

$$S_{red} = \int_0^\beta d\tau \Bigg[c_i^\dagger \frac{d}{d\tau} c_i + f_i^\dagger \frac{d}{d\tau} f_i + U c_i^\dagger c_i f_i^\dagger f_i + \sum_\nu \Delta(\nu) \frac{1}{\beta} \int_0^\beta d\tau' \left(c_i^\dagger c_i(\tau') e^{-i\nu(-\tau'+\tau)} + c_i^\dagger(\tau') c_i e^{i\nu(-\tau'+\tau)} \right) \Bigg] \quad (162)$$

Where the hybridization function $\Delta(\nu)$ is defined as in equation (62). The hybridization part of the action can easily be written in terms of frequency dependent Grassmann fields.

$$\sum_\nu \Delta(\nu) \frac{1}{\beta} \int_0^\beta d\tau \int_0^\beta d\tau' \left(c_i^\dagger c_i(\tau') e^{-i\nu(-\tau'+\tau)} + c_i^\dagger(\tau') c_i e^{i\nu(-\tau'+\tau)} \right) = \sum_\nu \Delta(\nu) \beta \left(c_i^\dagger(\nu) c_i(\nu) + c_i^\dagger(\nu) c_i(\nu) \right) \quad (163)$$

This simpler form will be used when relating the action of the Falicov-Kimball model and localized resonant level models.

6.2 Transformation of the Falicov-Kimball action

It is possible to add the hybridization part of the action for the resonant level model to the action for every single site of the Falicov-Kimball model and then subtract it again, leaving, of course, the Falicov-Kimball action unchanged.

$$S = \int_0^\beta d\tau \left[\sum_i \left(c_i^\dagger \frac{d}{d\tau} c_i + U c_i^\dagger c_i f_i^\dagger f_i \right) - t \sum_{\langle i,j \rangle} c_i^\dagger c_j \right] + \sum_{i,\nu} \Delta(\nu) \beta c_i^\dagger(\nu) c_i(\nu) - \sum_{i,\nu} \Delta(\nu) \beta c_i^\dagger(\nu) c_i(\nu) \quad (164)$$

This allows us to express the action of the Falicov-Kimball model as the sum of the actions of a set of resonant level models and the difference between the original kinetic and the hybridization terms.

$$S = \sum_i S_{RLM} - \int_0^\beta t \sum_{\langle i,j \rangle} c_i^\dagger c_j - \sum_{i,\nu} \Delta(\nu) \beta c_i^\dagger(\nu) c_i(\nu) \quad (165)$$

It is easy to see that since the hybridization contribution to the action is position independent, it will not change if a Fourier transformation in space is performed. This allows us to perform such a transformation, diagonalizing the kinetic term in the action. The kinetic term can then be also transformed into frequency space, yielding:

$$S = \sum_i S_{RLM} + \sum_{k,\nu} (\epsilon_k - \Delta(\nu)) c_k^\dagger(\nu) c_k(\nu) \quad (166)$$

A Hubbard-Stratanovich transformation allows us now to rewrite $e^{\sum_{k,\nu} (\epsilon_k - \Delta) c_k^\dagger(\nu) c_k(\nu)}$ as a Gaussian Grassmann integral over auxiliary fields $\zeta^{(\dagger)}$. Using the expression for Gaussian Grassmann integrals from [15],

$$\int \prod_i d\zeta_i^\dagger d\zeta_i \, e^{-\zeta_i^\dagger A_{ij} \zeta_j + \zeta_i^\dagger \eta_i + \eta_i^\dagger \zeta_i} = \det(A) e^{\eta_i^\dagger A_{ij}^{-1} \eta_j}, \quad (167)$$

allows us to rewrite

$$e^{\sum_{k,\nu}(\epsilon_k-\Delta(\nu))c_k^\dagger(\nu)c_k(\nu)} = \int \prod_{k,\nu} d\zeta_k^\dagger(\nu) d\zeta_k(\nu)\,(\epsilon_k-\Delta) e^{-\zeta_k^\dagger(\nu)\frac{1}{\epsilon_k-\Delta(\nu)}\zeta_k(\nu)+\zeta_k^\dagger(\nu)c_k(\nu)+c_k^\dagger(\nu)\zeta_k(\nu)}. \quad (168)$$

Then the c-electron part of the action of the system is written in terms of two different fields coupling to each other, c fields which appear only locally in the action and ζ fields, so called dual fermions [16], carrying the information about kinetic energy. A controlled approximation in the coupling between the fields is possible, resulting in the ζ fields interacting via many-particle Green's functions of local resonant level systems. The partition function for the system is then given by:

$$Z = F \int \left(\prod_{i,k} Dc_i^\dagger Dc_i Df_i^\dagger Df_i D\zeta_k^\dagger D\zeta_k \right) e^{-\sum_i S_{RLM}[c_i,c_i^\dagger,f_i,f_i^\dagger]-\sum_k \zeta_k^\dagger(\nu)\frac{1}{\epsilon_k-\Delta(\nu)}\zeta_k(\nu)+\zeta_k^\dagger(\nu)c_k(\nu)+c_k^\dagger(\nu)\zeta_k(\nu)}. \quad (169)$$

The factor F at the beginning of the expression originates from the Hubbard-Stratanovich Transformation performed, but can be neglected for the calculation of Green's functions as it cancels out due to the normalization anyway. The couplings between the original fermions and the newly introduced dual fermions,

$$\sum_k \zeta_k^\dagger(\nu)c_k(\nu) + c_k^\dagger(\nu)\zeta_k(\nu), \quad (170)$$

can be rewritten as sum over all lattice sites

$$\sum_i \zeta_i^\dagger(\nu)c_i(\nu) + c_i^\dagger(\nu)\zeta_i(\nu), \quad (171)$$

as a consequence of Parseval's theorem, because a summation over all values of k is performed. In this way, the localized resonant level systems provide a potential in which the dual fermions move.
Formally, the part

$$\int \prod_i Dc_i^\dagger Dc_i Df_i^\dagger Df_i\, e^{-S_{RLM}[c_i,c_i^\dagger,f_i,f_i^\dagger]+\zeta_i^\dagger(\nu)c_i(\nu)+c_i^\dagger(\nu)\zeta_i(\nu)} \quad (172)$$

is equivalent to the integrals appearing when introducing source fields to calculate Green's functions [12]. Thus, a controlled expansion in orders of the fields ζ_i and $\zeta_i^\dagger$ leads to many-body Green's functions coupling to them.

6.3 One Particle Irreducible approach

It has been argued [17], that the Dual Fermion approach, when truncating the expansion for the self-energy at the two-particle vertex level, can lead to inclusion of one-particle reducible contributions to the self-energy of the Hubbard model. While those contributions would be cancelled by others if one continued the expansion to the three-particle vertex level, a truncation at the two-particle vertex level leads to errors. The one particle irreducible ($1PI$) approach

allows for a transformation of the action, getting rid of the one-particle-reducible terms of two- and more particle vertices. Defining

$$Z_{RLM}\left[\zeta,\zeta^\dagger\right] = \int Dc^\dagger DcDf^\dagger Df e^{-S_{RLM}+\sum_\nu \zeta^\dagger(\nu)c(\nu)+c^\dagger(\nu)\zeta(\nu)}, \tag{173}$$

one can easily see that a formal differentiation of the integral above by the fields ζ and $\zeta^\dagger$ leads to factors $c^\dagger$ and c in the integrand, thus yielding the Green's functions of the system. The term Z_{RLM} allows for the definition of the generating functional of connected diagrams, W_{RLM}:

$$Z_{RLM}\left[\zeta,\zeta^\dagger\right] = e^{W_{RLM}\left[\zeta,\zeta^\dagger\right]}. \tag{174}$$

The problem with W_{RLM} is that, when differentiated with respect to ζ and $\zeta^\dagger$, it yields full, connected vertices, which contain reducible contributions. In dual fermion theory, one would expand W in orders of ζ and $\zeta^\dagger$, resulting in full local vertices appearing in the action (169). The inclusion of one-particle reducible contributions in the expansion can be thwarted by performing a suitable transformation before the differentiations. Note that on the two-particle level, the full, connected diagrams and the one-particle irreducible diagrams coincide, essentially due to particle conservation. This is, however, not the case for three- or higher-order diagrams. The one-particle irreducible generating functional Γ, is given by

$$\Gamma\left[\Phi^\dagger,\Phi\right] = W\left[\zeta,\zeta^\dagger\right] - \zeta^\dagger\left(\delta_{\zeta^\dagger}W\left[\zeta,\zeta^\dagger\right]\right) + \left(\delta_\zeta W\left[\zeta,\zeta^\dagger\right]\right)\zeta, \tag{175}$$

the Legendre transformation of W. Here, $\delta_{\zeta^{(\dagger)}}$ has been used as symbol for differentiation by $\zeta^{(\dagger)}$. The dependency of W on $\zeta^{(\dagger)}$ has been omitted when differentiated for better readability. The new fields introduced, $\Phi^{(\dagger)}$ are given by

$$\Phi = -\delta_{\zeta^\dagger}W\left[\zeta,\zeta^\dagger\right] \tag{176a}$$

$$\Phi^\dagger = \delta_\zeta W\left[\zeta,\zeta^\dagger\right]. \tag{176b}$$

The inverse transformation is defined by

$$\zeta = \delta_{\Phi^\dagger}\Gamma\left[\Phi,\Phi^\dagger\right] \tag{177a}$$

$$\zeta^\dagger = -\delta_\Phi\Gamma\left[\Phi,\Phi^\dagger\right]. \tag{177b}$$

Besides the transformation of the integrand, one should also transform the integration variables from $\zeta^{(\dagger)}$ to $\Phi^{(\dagger)}$. With Grassman integration, transformations of the integration variables are performed by the rule

$$d\Phi\ \delta_\zeta(\Phi) = d\zeta. \tag{178}$$

Thus, when transforming

$$d\zeta^\dagger d\zeta \to d\Phi^\dagger d\Phi, \tag{179}$$

a factor

$$\begin{vmatrix} \delta_\zeta(\Phi) & \delta_{\zeta^\dagger}(\Phi) \\ \delta_\zeta(\Phi^\dagger) & \delta_{\zeta^\dagger}(\Phi^\dagger) \end{vmatrix} \tag{180}$$

must be included in the integrand. In the following, we apply this transformation to the Falicov-Kimball model after the Hubbard-Stratanovich decoupling in equation (168).

$$Z = F\int\prod_k D\zeta_k^\dagger D\zeta_k\, e^{\sum_i W_{RLM\ i}\left[\zeta,\zeta^\dagger\right]-\sum_k \zeta_k^\dagger(\nu)\frac{1}{\epsilon_k-\Delta}\zeta_k(\nu)} \tag{181}$$

To this end, we insert source fields $\eta^{(\dagger)}$ for the original fermions.

$$Z\left[\eta,\eta^\dagger\right] = F\int\prod_{i,k} D\zeta_k^\dagger D\zeta_k\, e^{W_{RLM\ i}\left[\zeta+\eta,\zeta^\dagger+\eta^\dagger\right]-\zeta_k^\dagger(\nu)\frac{1}{\epsilon_k-\Delta}\zeta_k(\nu)} \tag{182}$$

A linear shift in the integration variables $\zeta^{(\dagger)}$ by $\eta^{(\dagger)}$ can easily be treated, yielding

$$Z\left[\eta,\eta^\dagger\right] = F\int D\zeta^\dagger D\zeta\, e^{W_{RLM}\left[\zeta_i,\zeta_i^\dagger\right]-\left(\zeta_k^\dagger(\nu)-\eta_k^\dagger(\nu)\right)\frac{1}{\epsilon_k-\Delta}(\zeta_k(\nu)-\eta_k(\nu))}. \tag{183}$$

It should be noted, that the local quantities W_{RLM} and Γ, when written in momentum space, scatter with equal amplitudes between all states which obey conservation of total momentum. Specifically, this means that up to second order in their fields, their k representation is given by

$$\sum_k \Psi_k^\dagger G_{loc}\Psi_k, \tag{184}$$

While up to fourth order it becomes

$$\frac{1}{2}\sum_{k,k',q}\Psi_k^\dagger\Psi_{k'}^\dagger V_{loc}\Psi_{k+q}\Psi_{k'-q}. \tag{185}$$

Here, $\Psi^{(\dagger)}$ are the fields associated with either W_{RLM} or Γ and V is the corresponding vertex (either the connected or 1PI vertex). Now, W_{RLM} can be replaced by it's Legendre transdorm Γ, substituting the integration variables as well.

$$Z\left[\eta,\eta^\dagger\right] = F\int\prod_{i,k} D\Phi_k^\dagger D\Phi_k$$
$$e^{\Gamma_i\left[\Phi,\Phi^\dagger\right]+(\delta_\Phi\Gamma)\Phi-\Phi^\dagger(\delta_{\Phi^\dagger}\Gamma)-\left(\eta_k^\dagger(\nu)+(\delta_{\Phi_k}\Gamma)\right)\frac{1}{\epsilon_k-\Delta}\left(\eta_k(\nu)-(\delta_{\Phi_k^\dagger}\Gamma)\right)}\det(M) \tag{186}$$

Another Hubbard-Stratanovich transformation allows for the replacement of the quadratic term $\left(\eta_k^\dagger(\nu)+\delta_{\Phi_k}\Gamma\right)\frac{1}{\epsilon_k-\Delta}\left(\eta_k(\nu)-\delta_{\Phi_k^\dagger}\Gamma\right)$. It turns out to be convenient to choose the multiplicative factor in the transformation in a fashion so as to get rid of remnants of $1/(\epsilon_k-\Delta)$ in the new mixed terms in the integrand. After the Hubbard-Stratanovich-transformation, the partition function of the system takes the form

$$Z\left[\eta,\eta^\dagger\right] = F'\int\prod_k D\Phi_k^\dagger D\Phi_k D\Psi_k^\dagger D\Psi_k e^{\sum_k\Psi_k^\dagger(\epsilon_k-\Delta)\Psi_k}$$
$$e^{\sum_i\Gamma_i\left[\Phi,\Phi^\dagger\right]+(\delta_{\Phi_i}\Gamma_i)\Phi_i-\Phi_i^\dagger(\delta_{\Phi_i^\dagger}\Gamma_i)-\left(\eta_i^\dagger(\nu)+(\delta_{\Phi_i}\Gamma)\right)\Psi_i-\Psi_i^\dagger\left(\eta_i(\nu)-(\delta_{\Phi_i^\dagger}\Gamma_i)\right)}\det(M). \tag{187}$$

It is possible to make the source fields couple symmetrically to the $\Psi^{(\dagger)}$ and $\Phi^{(\dagger)}$ fields and get rid of the terms $(\delta_\Phi\Gamma)\Phi$ and $\Phi^\dagger(\delta_{\Phi^\dagger}\Gamma)$ in the exponent by introducing a linear shift of $\Psi^{(\dagger)}$ by $\Phi^{(\dagger)}$.

$$\Psi^\dagger \to \Psi^\dagger + \Phi^\dagger \tag{188a}$$
$$\Psi \to \Psi + \Phi \tag{188b}$$

After the substitution, the generating functional reads:

$$Z\left[\eta,\eta^\dagger\right] = F' \int \prod_k D\Phi_k^\dagger D\Phi_k D\Psi_k^\dagger D\Psi_k e^{\sum_i \Gamma_i\left[\Phi,\Phi^\dagger\right]-(\delta_{\Phi_i}\Gamma_i)\Psi_i+\Psi_i^\dagger(\delta_{\Phi_i^\dagger}\Gamma_i)}$$
$$e^{\sum_k -\eta_k^\dagger(\nu)(\Psi_k+\Phi_k)-(\Psi_k^\dagger+\Phi_k^\dagger)\eta_k(\nu)+(\Psi_k^\dagger+\Phi_k^\dagger)(\epsilon_k-\Delta)(\Psi_k+\Phi_k)} \det(M) \quad (189)$$

Diagrammatically, this action can be interpreted as describing two particles, which can change their character freely via one-particle Green's functions. This can be seen from the term $(\Psi_k^\dagger + \Phi_k^\dagger)(\epsilon_k - \Delta)(\Psi_k + \Phi_k)$ which couples $\Phi^{(\dagger)}$ and $\Psi^{(\dagger)}$ fields. These particles interact via the terms $\Gamma\left[\Phi,\Phi^\dagger\right]$, $\Psi^\dagger(\delta_{\Phi^\dagger}\Gamma)$ and $(\delta_\Phi\Gamma)\Psi$. This means that terms of arbitrary order in the fields $\Phi^{(\dagger)}$ appear, while $\Psi^\dagger$ appears either in first order, or not at all. As discussed in [12], the contributions stemming from $\det(M)$ would lead to purely local terms and represent double-counting corrections, as they cancel corresponding purely local self-energy corrections. So far, all the transformations applied to the functional integral representation of the Falicov-Kimball action were exact. A widespread approximation is the consideration of terms up to the two-particle level only in the expansions of Γ and $\det(M)$. The expansion of Γ in second order in the fields $\Phi^{(\dagger)}$ yields the inverse of the local DMFT Green's function, G_{loc}^{-1} and the one particle irreducible, full local vertex F in fourth order.

$$\Gamma_i\left[\Phi,\Phi^\dagger\right] =$$
$$\mathcal{C} + \sum_\nu \Phi_i^\dagger(\nu) G_{loc}^{-1}(\nu)\Phi_i(\nu) + \frac{1}{4}\sum_{\nu,\nu',\omega} \Phi_i^\dagger(\nu+\omega)\Phi_i^\dagger(\nu')F^{\nu\nu'\omega}\Phi_i(\nu'+\omega)\Phi_i(\nu) + \mathcal{O}\left(\Phi^{(\dagger)6}\right) \quad (190)$$

In this context, $\mathcal{C}$ is $\ln(Z_{RLM})$ but the value is irrelevant, as it cancels out from all expectation values anyway. The terms containing functional derivatives of Γ give very similar expressions, albeit replacing one of the $\Phi^{(\dagger)}$ fields by $\Psi^{(\dagger)}$:

$$-\left(\delta_{\Phi_i}\Gamma_i\left[\Phi,\Phi^\dagger\right]\right)\Psi_i =$$
$$\sum_\nu \Phi_i^\dagger(\nu) G_{loc}^{-1}(\nu)\Psi_i(\nu) + \frac{1}{2}\sum_{\nu,\nu',\omega} \Phi_i^\dagger(\nu+\omega)\Phi_i^\dagger(\nu')F^{\nu\nu'\omega}\Phi_i(\nu'+\omega)\Psi_i(\nu) + \mathcal{O}\left(\Phi^{(\dagger)5}\Psi\right) \quad (191)$$

$$\Psi_i^\dagger\left(\delta_{\Phi_i^\dagger}\Gamma_i\left[\Phi,\Phi^\dagger\right]\right) =$$
$$\sum_\nu \Psi_i^\dagger(\nu) G_{loc}^{-1}(\nu)\Phi_i(\nu) + \frac{1}{2}\sum_{\nu,\nu',\omega} \Phi_i^\dagger(\nu+\omega)\Psi_i^\dagger(\nu')F^{\nu\nu'\omega}\Phi_i(\nu'+\omega)\Phi_i(\nu) + \mathcal{O}\left(\Phi^{(\dagger)5}\Psi^\dagger\right) \quad (192)$$

In total, one gets quadratic contributions to the action, coupling $\Phi^{(\dagger)}$ and $\Psi^{(\dagger)}$ via ${G_k}^{-1}$ or ${G_k}^{-1} - G_{loc}^{-1}$. The full local vertex assumes the role of a bare interaction for the system.

6.3.1 Ladder approximation for the one particle irreducible approach

As the bare interaction for the $1PI$ approach is known to be the full local vertex of the associated resonant level model, a diagrammatic expansion of the $1PI$ system can be conducted. It should be noted that the decomposition of the full local vertex into the different two-particle irreducible ones, with respect to real electrons, bears no meaning for the $1PI$ formalism. The full vertex is considered to be the bare interaction, thus even being fully irreducible with respect to the dual electrons. This justifies building ladders with F_{loc} as basic building block. It should be noted, however, that such a ladder construction is equivalent to the one conducted with Γ_{ph}

and G_{DMFT}. The corresponding Bethe-Salpeter equation in the particle-hole channel, adapted from [12] is given by:

$$F_q^{\nu\nu'\omega} = F_{loc}^{\nu\nu'\omega} - \frac{1}{\beta}\sum_{\nu_1,k_1} F_{loc}^{\nu\nu_1\omega} G_{red}(\nu_1,k_1)G_{red}(\nu_1+\omega,k_1+q)F_q^{\nu_1\nu'\omega}. \tag{193}$$

Where G_{red} is given by

$$G_{red}(\nu,k) = G(\nu,k) - G_{loc}(\nu), \tag{194}$$

i.e. the difference between the DMFT Green's function and the local Green's function of the RLM problem. F_{loc} is already known to be, for the Falicov-Kimball model, of the form

$$F_{loc}^{\nu\nu'\omega} = (\delta_{\omega,0} - \delta_{\nu,\nu'})a(\nu)a(\nu'+\omega). \tag{195}$$

Where $a(\nu)$ is defined in equation (86). For $\omega \neq 0$, the equation becomes

$$F_q^{\nu\nu'\omega\neq 0} = -\delta_{\nu,\nu'}a(\nu)a(\nu+\omega) + \frac{1}{\beta}\sum_{k_1} a(\nu)a(\nu+\omega)G_{red}(\nu,k_1)G_{red}(\nu+\omega,k_1+q)F_q^{\nu\nu'\omega\neq 0}. \tag{196}$$

It can be rewritten as

$$F_q^{\nu\nu'\omega\neq 0}\left(1 - a(\nu)a(\nu+\omega)\frac{1}{\beta}\sum_{k_1} G_{red}(\nu,k_1)G_{red}(\nu+\omega,k_1+q)\right) = -\delta_{\nu,\nu'}a(\nu)a(\nu+\omega). \tag{197}$$

Thus justifying the definition of the function u as :

$$u(\nu,\omega,q) = \frac{a(\nu)a(\nu+\omega)}{1 - a(\nu)a(\nu+\omega)\frac{1}{\beta}\sum_{k_1} G_{red}(\nu,k_1)G_{red}(\nu+\omega,k_1+q)}, \tag{198}$$

which yields, with $a(\nu)$ from equation (86):

$$u(\nu,\omega,q) = \frac{\beta(\Sigma(\nu)-U)\Sigma(\nu)(\Sigma(\nu+\omega)-U)\Sigma(\nu+\omega)}{p_1p_2U^2 - (\Sigma(\nu)-U)\Sigma(\nu)(\Sigma(\nu+\omega)-U)\Sigma(\nu+\omega)\sum_{k_1} G_{red}(\nu,k_1)G_{red}(\nu+\omega,k_1+q)} \tag{199}$$

when inserting the explicit expression for a. This allows for $F_q^{\nu\nu'\omega\neq 0}$ to be written as:

$$F_q^{\nu\nu'\omega\neq 0} = -\delta_{\nu,\nu'}u(\nu,\omega,q). \tag{200}$$

As next step, the case $\omega = 0$ needs to be investigated. Without loss of generality, $F_q^{\nu\nu'\omega}$ can be assumed to be of the form

$$F_q^{\nu\nu'\omega} = \delta_{\omega,0}f(\nu,\nu',q) - \delta_{\nu,\nu'}u(\nu,\omega,q), \tag{201}$$

where f is some function which needs to be determined by evaluating the Bethe-Salpeter equation (193) for the case $\omega = 0$.

$$f(\nu,\nu',q) - \delta_{\nu,\nu'}u(\nu,0,q) = (1-\delta_{\nu,\nu'})a(\nu)a(\nu') - \frac{1}{\beta}\sum_{\nu_1 k_1}(1-\delta_{\nu,\nu_1})a(\nu)a(\nu_1)G_{red}(\nu_1,k_1)G_{red}(\nu_1,k_1+q)\left(f(\nu_1,\nu',q) - \delta_{\nu_1,\nu'}u(\nu',0,q)\right) \tag{202}$$

Evaluation of the sum gives rise to four terms.

$$\begin{aligned} f(\nu,\nu',q) - \delta_{\nu,\nu'}u(\nu,0,q) = (1-\delta_{\nu,\nu'})a(\nu)a(\nu') \\ - \frac{1}{\beta}\sum_{\nu_1 k_1} a(\nu)a(\nu_1)G_{red}(\nu_1,k_1)G_{red}(\nu_1,k_1+q)f(\nu_1,\nu',q) \\ + a(\nu)a(\nu)f(\nu,\nu',q)\frac{1}{\beta}\sum_{k_1} G_{red}(\nu,k_1)G_{red}(\nu,k_1+q) \\ + a(\nu)a(\nu')u(\nu',0,q)\frac{1}{\beta}\sum_{k_1} G_{red}(\nu',k_1)G_{red}(\nu',k_1+q) \\ - \delta_{\nu,\nu'}a(\nu)a(\nu)u(\nu,0,q)\frac{1}{\beta}\sum_{k_1} G_{red}(\nu,k_1)G_{red}(\nu,k_1+q). \end{aligned} \tag{203}$$

The terms that are proportional to $\delta_{\nu,\nu'}$ in equation (203) cancel each other, as can be easily verified from equation (198) for $\omega = 0$. This does not come as a surprise since those are exactly the terms constituting the equation for $\omega \neq 0$, which is fulfilled. The remaining terms are:

$$\begin{aligned} f(\nu,\nu',q) = a(\nu)a(\nu') - a(\nu)\frac{1}{\beta}\sum_{\nu_1 k_1} a(\nu_1)G_{red}(\nu_1,k_1)G_{red}(\nu_1,k_1+q)f(\nu_1,\nu',q)+ \\ a(\nu)a(\nu)f(\nu,\nu',q)\frac{1}{\beta}\sum_{k_1} G_{red}(\nu,k_1)G_{red}(\nu,k_1+q)+a(\nu)a(\nu')u(\nu',0,q)\frac{1}{\beta}\sum_{k_1} G_{red}(\nu',k_1)G_{red}(\nu',k_1+q) \end{aligned} \tag{204}$$

It is possible to solve this equation in a very similar fashion to the *ph*-ladder in section 5.2.2. To do so, the terms have to be rearranged:

$$\begin{aligned} \left(1 - a^2(\nu)\frac{1}{\beta}\sum_{k_1} G_{red}(\nu,k_1)G_{red}(\nu,k_1+q)\right) f(\nu,\nu',q) = a(\nu)\cdot \\ \left(a(\nu')\left(1 + u(\nu',0,q)\frac{1}{\beta}\sum_{k_1} G_{red}(\nu',k_1)G_{red}(\nu',k_1+q)\right) - \right. \\ \left. \frac{1}{\beta}\sum_{\nu_1 k_1} a(\nu_1)G_{red}(\nu_1,k_1)G_{red}(\nu_1,k_1+q)f(\nu_1,\nu',q)\right) \end{aligned} \tag{205}$$

The right hand side of equation (205) factorizes into a part depending on ν and a part depending on ν'. This implies that the left hand side of the equation has to do the same. This means that f has to factorize as well. It is convenient to assume a symmetric factorization for f:

$$f(\nu,\nu',q) = b(\nu,q)b(\nu',q) \tag{206}$$

Note that this function b is different to the function with the same name appearing in section 5.2.2. Inserting this expression into the Bethe-Salpeter equation gives the condition

$$b(\nu,q) = C_q \frac{a(\nu)}{1 - a(\nu)a(\nu)\frac{1}{\beta}\sum_{k_1} G_{red}(\nu,k_1)G_{red}(\nu,k_1+q)}. \tag{207}$$

The Bethe-Salpeter equation (205) then gives the condition for C_q:

$$C_q^2 = \frac{1}{1 + \sum_{\nu_1} \frac{a(\nu_1)a(\nu_1)\frac{1}{\beta}\sum_{k_1} G_{red}(\nu_1,k_1)G_{red}(\nu_1,k_1+q)}{1 - a(\nu_1)a(\nu_1)\frac{1}{\beta}\sum_{k_1} G_{red}(\nu_1,k_1)G_{red}(\nu_1,k_1+q)}} \tag{208}$$

The structure of the equations leading to the resulting full ladder vertex for the $1PI$ (and dual) fermions is very similar to the *ph*-ladder for the real *c*-electrons. One can indeed show, that the two are equivalent. Also, for the dual fermions, the full local vertex of the real electrons is used as an approximation for the *ph*-irreducible, local vertex. The full dual electron vertex (201) in the ladder approximation is given by:

$$F_q^{\nu,\nu',\omega} = \delta_{\omega,0} C_q^2 \frac{a(\nu)}{1 - a(\nu)a(\nu)\frac{1}{\beta}\sum_{k_1} G_{red}(\nu,k_1)G_{red}(\nu,k_1+q)} \frac{a(\nu')}{1 - a(\nu')a(\nu')\frac{1}{\beta}\sum_{k_1} G_{red}(\nu',k_1)G_{red}(\nu',k_1+q)} - \delta_{\nu,\nu'} u(\nu,\omega,q). \quad (209)$$

6.3.2 $1PI$ corrections for the self energy

In [12], an expansion for the real electron self-energy within $1PI$ theory was derived. This was done for the Hubbard model, but the same derivation is also applicable to the Falicov-Kimball model, as only a dispersion relation and the full local vertex within a $DMFT$ calculation are needed as input, putting no constraints on the actual nature of the interaction within the original system. The corrections for the self energy are given by:

$$\Sigma_1^{(1)}(\nu,k) = -\frac{2}{\beta^2}\sum_{\nu_1,\omega,k_1,q} F_{loc}^{\nu\nu_1\omega} G_{red}(\nu_1,k_1)G_{red}(\nu_1+\omega,k_1+q)F_q^{\nu_1\nu\omega}G_{red}(\nu+\omega,k+q) \quad (210a)$$

$$\Sigma_1^{(2)}(\nu,k) = \frac{1}{\beta^2}\sum_{\nu_1,\omega,k_1,q} F_{loc}^{\nu\nu_1\omega} G_{red}(\nu_1,k_1)G_{red}(\nu_1+\omega,k_1+q)F_{loc}^{\nu_1\nu\omega}G_{red}(\nu+\omega,k+q) \quad (210b)$$

$$\Sigma_2(\nu) = -\frac{2}{\beta^2}\sum_{\nu_1,\omega,k_1,q} F_{loc}^{\nu\nu_1\omega} G_{red}(\nu_1,k_1)G_{red}(\nu_1+\omega,k_1+q)F_q^{\nu_1\nu\omega}G_{loc}(\nu+\omega) \quad (210c)$$

The sum over the three terms gives the total correction to the self-energy within the $1PI$ theory when restricting oneself to inclusion of two particles vertices only. The term $\Sigma_1^{(1)}(\nu,k)$ is responsible for the non-local corrections and $\Sigma_2(\nu)$ gives corrections to the local, k-independent, self-energy. $\Sigma_1^{(2)}(\nu,k)$ accounts for double counting of the second-order terms in $\Sigma_1^{(1)}(\nu,k)$. Equation (193) allows for rewriting

$$-\frac{1}{\beta}\sum_{\nu_1,k_1} F_{loc}^{\nu\nu_1\omega} G_{red}(\nu_1,k_1)G_{red}(\nu_1+\omega,k_1+q)F_q^{\nu_1\nu\omega} = F_q^{\nu\nu\omega} - F_{loc}^{\nu\nu\omega}. \quad (211)$$

The corrections can then be written as:

$$\Sigma_1^{(1)}(\nu,k) = \frac{2}{\beta}\sum_{\omega,q}\left(F_q^{\nu\nu\omega} - F_{loc}^{\nu\nu\omega}\right)G_{red}(\nu+\omega,k+q) \quad (212a)$$

$$\Sigma_1^{(2)}(\nu,k) = \frac{1}{\beta^2}\sum_{\nu_1,\omega,k_1,q} F_{loc}^{\nu\nu_1\omega} G_{red}(\nu_1,k_1)G_{red}(\nu_1+\omega,k_1+q)F_{loc}^{\nu_1\nu\omega}G_{red}(\nu+\omega,k+q) \quad (212b)$$

$$\Sigma_2(\nu) = \frac{2}{\beta}\sum_{\omega,q}\left(F_q^{\nu\nu\omega} - F_{loc}^{\nu\nu\omega}\right)G_{loc}(\nu+\omega). \quad (212c)$$

Since F_{loc} does not depend on q, and the sum over all values of k of G_{red} equals zero per definitionem, the local vertex can be dropped from equation (212a). Inserting the explicit

expressions for F_q and F_{loc} yields, after some simplifications:

$$\Sigma_1^{(1)}(\nu,k) = \frac{2}{\beta}\sum_q C_q^2 \frac{a^2(\nu)}{\left(1-a^2(\nu)\frac{1}{\beta}\sum_{k_1} G_{red}(\nu,k_1)G_{red}(\nu,k_1+q)\right)^2} G_{red}(\nu,k+q) - \frac{2}{\beta}\sum_{q,\nu_1} \frac{a(\nu)a(\nu_1)}{1-a(\nu)a(\nu_1)\frac{1}{\beta}\sum_{k_1} G_{red}(\nu,k_1)G_{red}(\nu_1,k_1+q)} G_{red}(\nu_1,k+q) \quad (213)$$

$$\Sigma_1^{(2)}(\nu,k) = \frac{2}{\beta}\sum_{\nu_1,k_1,q} a^2(\nu)a^2(\nu_1)G_{red}(\nu_1,k_1)G_{red}(\nu_1,k_1+q)G_{red}(\nu,k+q) - \frac{2}{\beta}\sum_{k_1,q} a^4(\nu)G_{red}(\nu,k_1)G_{red}(\nu,k_1+q)G_{red}(\nu,k+q) \quad (214)$$

$$\Sigma_2(\nu) = \frac{2}{\beta}\sum_q C_q^2 \frac{a^2(\nu)}{\left(1-a^2(\nu)\frac{1}{\beta}\sum_{k_1} G_{red}(\nu,k_1)G_{red}(\nu,k_1+q)\right)^2} G_{loc}(\nu) - \frac{2}{\beta}\sum_{q,\nu_1} \frac{a(\nu)a(\nu_1)}{1-a(\nu)a(\nu_1)\frac{1}{\beta}\sum_{k_1} G_{red}(\nu,k_1)G_{red}(\nu_1,k_1+q)} G_{loc}(\nu_1) + \frac{2}{\beta}\sum_{\nu_1} a(\nu_1)G_{loc}(\nu_1)a(\nu) - \frac{2}{\beta}a^2(\nu)G_{loc}(\nu). \quad (215)$$

6.3.3 Numerical results for the self-energy corrections

A numerical evaluation of these equations is possible, allowing for description of effects beyond purely local correlations in the c-electron self-energy. Below, results for $1PI$ corrections of the self energy on a cubic lattice with nearest neighbour hoping are given. The calculations were performed based on converged DMFT calculations at (fixed) f-density $n_f = 1/2$. In particular, the behaviour in the vicinity of the transition to the charge ordered phase has been investigated.

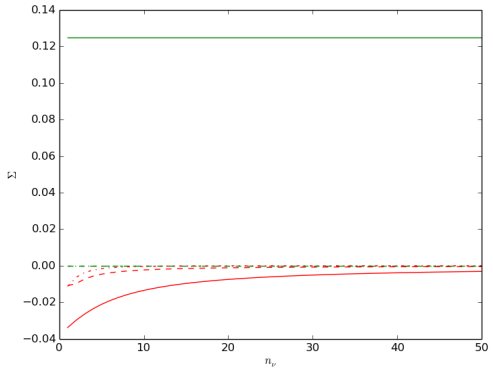

Figure 29: $1PI$ corrections to the self-energy near the phase transition

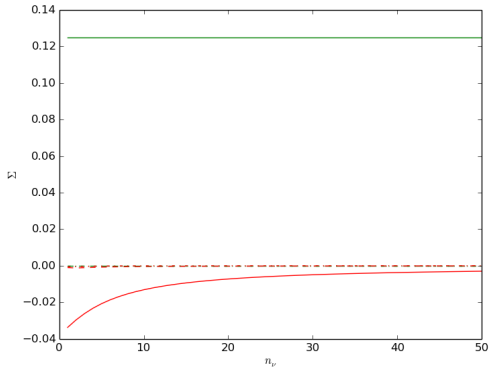

Figure 30: $1PI$ corrections for the self-energy at a slightly higher temperature

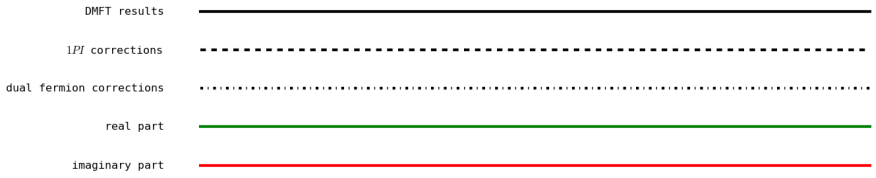

In figure 29 and 30, the real and imaginary parts of the DMFT-self-energy, the dual-fermion and the $1PI$ corrections to the self-energy at the k-point $(0, \pi/2, \pi)$ are plotted as functions of the fermionic Matsubara frequency ν. The dual-fermion corrections are the same as the $1PI$-ones, just neglecting $\Sigma_2(\nu)$. (Note that only the self-energy corrections for the dual fermions are considered, without transforming the dual self-energy to a real fermion self-energy) The calculations were performed at $U = 0.25$ and $\beta = 62.15$ and 60 respectively. Green lines show real parts and red imaginary ones. Full lines give the DMFT-self-energy, dashed ones the corrections within a $1PI$-ph-ladder approximation and chain-dotted ones the corrections obtained from a Dual-Fermion ph-ladder. One can see that the real part of the self-energy is fixed at $U/2 = 0.125$ and the corrections give 0. This is a consequence of the particle-hole symmetry for the half-filled Falicov-Kimball model. The corrections to the imaginary part are small when one is far enough away from the phase transition, but increase in value when approaching it. This indicates the enhanced nonlocal scattering of electrons at charge fluctuations when approaching the charge density wave instability. The $1PI$ corrections are larger in magnitude than the Dual-Fermion ones, which is a consequence of the allowed propagators. The high-frequency behaviour is also different: While the $1PI$-corrections have a contribution of order $1/\nu$, the dual fermion corrections decay faster as the frequency increases.
For the numerical evaluation of the self-energy corrections, the summands were distributed as follows: The terms which involve summations over ν_1 but which are not part of $\Sigma^{(2)}$, originally stemming from terms proportional to $\delta(\nu, \nu')$, i.e. the second term on the right hand side of

equation (213) and the fourth from (215) , were expressed in terms of:

$$\Sigma_k^{\nu,\nu}(\nu,k) = \frac{2}{\beta}\sum_{q,\nu_1} \frac{a^2(\nu)a^2(\nu_1)\frac{1}{\beta}\sum_{k_1} G_{red}(\nu,k_1)G_{red}(\nu_1,k_1+q)}{1-a(\nu)a(\nu_1)\frac{1}{\beta}\sum_{k_1} G_{red}(\nu,k_1)G_{red}(\nu_1,k_1+q)} G(\nu_1,k+q), \tag{216a}$$

$$\Sigma_{loc}^{\nu,\nu}(\nu) = \frac{2}{\beta}\sum_{q,\nu_1} \frac{a^2(\nu)a^2(\nu_1)\frac{1}{\beta}\sum_{k_1} G_{red}(\nu,k_1)G_{red}(\nu_1,k_1+q)}{1-a(\nu)a(\nu_1)\frac{1}{\beta}\sum_{k_1} G_{red}(\nu,k_1)G_{red}(\nu_1,k_1+q)} G_{loc}(\nu_1). \tag{216b}$$

Here, the name ν,ν implies the origin of the terms. The enumerator stems from the difference

$$\frac{2}{\beta}\sum_{q,\nu_1} \frac{a(\nu)a(\nu_1)}{1-a(\nu)a(\nu_1)\frac{1}{\beta}\sum_{k_1} G_{red}(\nu,k_1)G_{red}(\nu_1,k_1+q)} G(\nu_1,k+q) - \frac{2}{\beta}\sum_{q,\nu_1} a(\nu_1)G(\nu_1,k+q)a(\nu), \tag{217}$$

which can be written as

$$\frac{2}{\beta}\sum_{q,\nu_1}\left(\frac{a(\nu)a(\nu_1)}{1-a(\nu)a(\nu_1)\frac{1}{\beta}\sum_{k_1} G_{red}(\nu,k_1)G_{red}(\nu_1,k_1+q)} - a(\nu)a(\nu_1)\right) G(\nu_1,k+q), \tag{218}$$

when using $G_{red}(\nu,q) = G(\nu,q) - G_{loc}(\nu)$ and $\sum_q G(\nu,q) = G_{loc}(\nu)$. This yields (216a) when expanding to the same denominator and the same is true when using the local Green's function G_{loc} instead of G. While the *loc*-terms are not needed for calculating the $1PI$-corrections, they must be subtracted to arrive at the dual-fermion ones. The terms turned out not to change very much when varying the k-mesh for the summation or the number of included Matsubara frequencies, as long as a sufficient number was taken into account (about 50 frequencies and 17^3 k-points).
The two terms containing C_q^2 (i.e. the first terms on the right hand sides of equations (213) and (215)), originating from terms originally proportional to $\delta_{\omega,0}$ were calculated together, specifically

$$\Sigma_k^{\omega,0}(\nu,k) = \frac{2}{\beta}\sum_q C_q^2 \frac{a^2(\nu)}{\left(1-a^2(\nu)\frac{1}{\beta}\sum_{k_1} G_{red}(\nu,k_1)G_{red}(\nu,k_1+q)\right)^2} G(\nu,k+q), \tag{219a}$$

$$\Sigma_{loc}^{\omega,0}(\nu) = \frac{2}{\beta}\sum_q C_q^2 \frac{a^2(\nu)}{\left(1-a^2(\nu)\frac{1}{\beta}\sum_{k_1} G_{red}(\nu,k_1)G_{red}(\nu,k_1+q)\right)^2} G_{loc}(\nu). \tag{219b}$$

The computational time for the $\Sigma^{\omega,0}$-corrections for a given k-value scales like $N_\nu^2 N_k^2$, where N_ν is the total number of Matsubara-frequencies taken into account and N_k is the number of k-points on the mesh used for the summations. The number of Matsubara frequencies turned out not to be critical as a sufficient number could be easily included in the calculation. The number of k-points could not be adjusted as easily, as a cubic lattice was assumed and $N_k \propto n_k^3$, with n_k being the number of different k-points in a given direction. The lattice could only be increased in size by increments of 4 in every direction as $\pi/2$ was needed as point on the mesh. Below, figure 31 shows the dependency of the imaginary part of the $1PI$ corrections to the

self-energy for the k-point $(0, \pi/2, \pi)$, $\Sigma^{1PI}(\nu_1, (0, \pi/2, \pi))$ at the first Matsubara frequency for $U = 0.5, \mu = 0.25$ and $\beta = 30.28$ as function of $1/n_k$, using constant values for the remaining summands $\Sigma^{\nu,\nu}$ and Σ^{loc}.

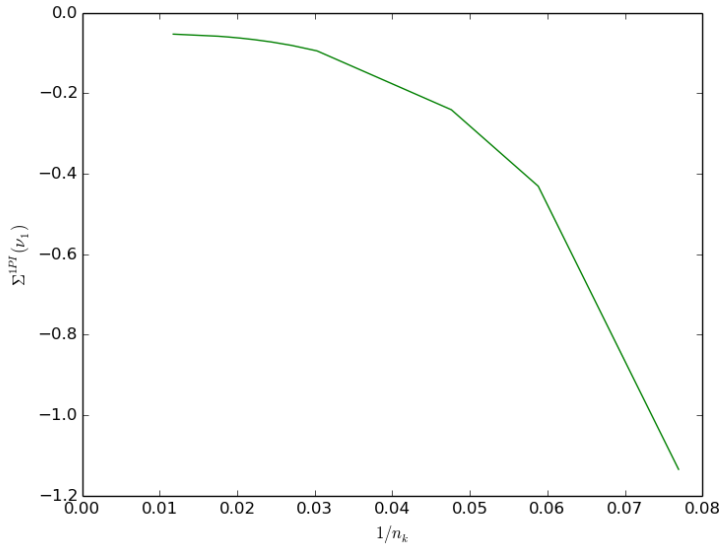

Figure 31: Dependency of $1PI$ corrections to the imaginary part of the self-energy on the inverse number k-points per direction

One can see that a large amount of k-points is needed to predict the behaviour of $\Sigma^{\omega,0}$. This stems from the multiplicative factors C_q^2 which become very large at specific values of q. If the k-point mesh is not fine enough, those q-points are weighted too much and dominate the whole sum.
The last terms (i.e. the ones from quation (214)) to be calculated were

$$\Sigma_k^{loc}(\nu, k) = \frac{2}{\beta} \sum_{\nu_1, k_1, q} a^2(\nu) a^2(\nu_1) G_{red}(\nu_1, k_1) G_{red}(\nu_1, k_1 + q) G(\nu, k + q) - \frac{2}{\beta} \sum_{k_1, q} a^4(\nu) G_{red}(\nu, k_1) G_{red}(\nu, k_1 + q) G(\nu, k + q), \quad (220a)$$

$$\Sigma_{loc}^{loc}(\nu) = \frac{2}{\beta} \sum_{\nu_1, k_1, q} a^2(\nu) a^2(\nu_1) G_{red}(\nu_1, k_1) G_{red}(\nu_1, k_1 + q) G_{loc}(\nu) - \frac{2}{\beta} \sum_{k_1, q} a^4(\nu) G_{red}(\nu, k_1) G_{red}(\nu, k_1 + q) G_{loc}(\nu). \quad (220b)$$

Leaving only the term

$$-\frac{2}{\beta} a^2(\nu) G_{loc}(\nu) \quad (221)$$

from equation (215) to be added. It is physically justifiable to treat the Σ^{loc} terms separately, as they correspond to diagrams that take care of double counting in the $1PI$-ladder. They can be treated by a simple summation, and do not change very much upon increasing either n_k or N_ν.

7 Conclusion

In this thesis, local vertex functions for the Falicov-Kimball model were calculated analytically within DMFT, including the full vertex, the vertices irreducible in a given channel and the fully irreducible vertex. Based on the full local vertex, the $1PI$-theory was applied to calculate non-local corrections for the self-energy.
In chapter 3, general features of the Falicov-Kimball model have been discussed, including perturbation theory for the disordered phase and a justification of the lattice model's tendency towards checkerboard ordering. Also, a brief introduction to the Green's function in quantum field theory is given, as a necessary tool for most of the calculations performed in this thesis.
Dynamical mean field theory has successfully been applied to the Falicov-Kimball model in chapter 4. The full local vertex was calculated and a decomposition into irreducible ones was performed. To the best of my knowledge, this is the first time the full decomposition was performed analytically. From the divergence of the particle-particle susceptibility in DMFT, the phase transition towards an ordered state was determined. Trying to describe the behaviour near the phase transition better, Feynman-diagrammatic methods were employed, including some correlations beyond purely mean values of interaction in the treatment.
Chapter 5 is devoted to a discussion of the local vertices obtained from DMFT and ladder approximations of the full vertex based on irreducible vertices. The full vertex and the irreducible vertices were expressed in closed form and their general features were discussed. Some of the analytical features of the vertices exist in similar form for some fully interacting models, like the Hubbard model in the atomic limit. Also, divergences in the irreducible vertices where observed, appearing in a similar form for the Hubbard model. Thus, the results can provide a useful comparison.
The application of the $1PI$-theory to the Falicov-Kimball model yielded analytical results when a ladder approximation was performed as shown in chapter 6. Because a mayor part of the calculations was performed without falling back to numerical methods, the results can be interpreted more easily. This may allow for a better understanding of the behaviour of the employed methods. The thesis is concluded by a numerical evaluation of the corrections to the self-energy, including a brief discussion of convergence behaviour for the different contributions.

References

[1] L. M. Falicov and J. C. Kimball. Simple model for semiconductor-metal transistions: SmB_6 and transition-metal oxides. *Phys. Rev. Lett.*, 1969.

[2] J. Hubbard. Electron correlations in narrow energy bands. *Proc. Phys. Soc. London*, 1963.

[3] Freericks J.K. and Zlatić V. Exact dynamical mean-field theory of the Falicov-Kimball model. *Rev. Mod. Phys.*, 2003.

[4] Brandt U. and Schmidt R. Ground state properties of a spinless Falicov-Kimball model. *Zeitschrift f. Physik B*, 1987.

[5] Brandt U. and Schmidt R. Exact results for the distribution of the f-level ground state occupation in the spinless Falicov-Kimball model. *Zeitschrift f. Physik B*, 1986.

[6] T. D. Stanescu and G. Kotliar. Strong coupling theory for interacting lattice models. *Phys. Rev. B*, 2004.

[7] K. Held. Electronic structure calculations using dynamical mean field theory, cond-mat/0511293, based on the habilitation thesis, 2004.

[8] Georges A., Kotliar G., Krauth W., and Rozenberg M. J. Dynamical mean-field theory of strongly correlated fermion systems and the limit of infinite dimensions. *Rev. Mod. Phys.*, 1996.

[9] Metzner W. and Vollhardt D. Correlated lattice fermions in $d = \infty$ dimensions. *Phys. Rev. Lett.*, 1989.

[10] Brandt U. and Mielsch C. Thermodynamics and correlation functions of the Falicov-Kimball model in large dimensions. *Zeitschrift f. Physik B*, 1989.

[11] A. Abrikosov, L. Gorkov, and Dzyaloshinsky. *Methods of Quantum Field Theory in Statistical Physics*. Dover, 1975.

[12] G. Rohringer. *New routes towards a theoretical treatment of nonlocal electronic correlations*. PhD thesis, TU Wien, 2013.

[13] Schäfer T., Rohringer G., Gunnarsson O., Ciuchi S., Sangiovanni G., and Toschi A. Divergent precursors of the Mott-Hubbard transition at the two-particle level. *Phys. Rev. Lett.*, 2013.

[14] V. Janis and V. Pokorny. Critical metal-insulator transition and divergence in a two-particle irreducible vertex in disordered and interacting electron systems. *Phys. Rev. B*, 2014.

[15] Negele J. W. and Orland H. *Quantum Many-Particle Systems*. Addison-Wesley Publishing Company, 1988.

[16] A. N. Rubtsov, M. I. Katsnelson, and A. I. Lichtenstein. Dual fermion approach to nonlocal correlations in the Hubbard model. *Phys. Rev. B*, 2008.

[17] A. A. Katanin. The effect of six-point one-particle reducible local interactions in the dual fermion approach. *J. Phys. A*, 2013.